

**ISTANBUL TECHNICAL UNIVERSITY ★ GRADUATE SCHOOL**

**OPTIMIZED POWER CONTROL STRATEGY  
FOR A PROTON EXCHANGE MEMBRANE FUEL CELL SYSTEM**

**M.Sc. THESIS**

**Ömer Burak SARIÇAY**

**Department of Control and Automation Engineering**

**Control and Automation Engineering Programme**

**JUNE 2024**



**ISTANBUL TECHNICAL UNIVERSITY ★ GRADUATE SCHOOL**

**OPTIMIZED POWER CONTROL STRATEGY  
FOR A PROTON EXCHANGE MEMBRANE FUEL CELL SYSTEM**

**M.Sc. THESIS**

**Ömer Burak SARIÇAY  
(504211115)**

**Department of Control and Automation Engineering**

**Control and Automation Engineering Programme**

**Thesis Advisor: Prof. Dr. Fikret ÇALIŞKAN**

**JUNE 2024**



**İSTANBUL TEKNİK ÜNİVERSİTESİ ★ LİSANSÜSTÜ EĞİTİM ENSTİTÜSÜ**

**PROTON DEĞİŞİM MEMBRANLI YAKIT HÜCRESİ SİSTEMİ İÇİN  
OPTİMİZE EDİLMİŞ GÜÇ KONTROL STRATEJİSİ**

**YÜKSEK LİSANS TEZİ**

**Ömer Burak SARIÇAY  
(504211115)**

**Kontrol ve Otomasyon Mühendisliği Anabilim Dalı**

**Kontrol ve Otomasyon Mühendisliği Programı**

**Tez Danışmanı: Prof. Dr. Fikret ÇALIŞKAN**

**HAZİRAN 2024**



Ömer Burak SARIÇAY, a M.Sc. student of ITU Graduate School student ID 504211115 successfully defended the thesis entitled “OPTIMIZED POWER CONTROL STRATEGY FOR A PROTON EXCHANGE MEMBRANE FUEL CELL SYSTEM”, which he/she prepared after fulfilling the requirements specified in the associated legislations, before the jury whose signatures are below.

**Thesis Advisor :**    **Prof. Dr. Fikret ÇALIŞKAN** .....  
Istanbul Technical University

**Jury Members :**    **Assoc. Prof. Dr. Mehmet Suha YAZICI** .....  
Istanbul Technical University

**Asst. Prof. Dr. Claudia Fernanda YAŞAR** .....  
Yıldız Technical University

**Date of Submission :**    **14 May 2024**

**Date of Defense :**        **10 June 2024**





*To my family,*



## **FOREWORD**

I would like to thank Prof. Dr. Fikret Çalışkan for his supervision, guidance, and unwavering support throughout this endeavor. I would like to thank my executives and friends from AVL Research and Engineering Turkey for their valuable support.

June 2024

Ömer Burak SARIÇAY  
(Systems Engineer)





## TABLE OF CONTENTS

	<u>Page</u>
<b>FOREWORD</b> .....	<b>ix</b>
<b>TABLE OF CONTENTS</b> .....	<b>xi</b>
<b>ABBREVIATIONS</b> .....	<b>xiii</b>
<b>SYMBOLS</b> .....	<b>xv</b>
<b>LIST OF TABLES</b> .....	<b>xvii</b>
<b>LIST OF FIGURES</b> .....	<b>xix</b>
<b>SUMMARY</b> .....	<b>xxi</b>
<b>ÖZET</b> .....	<b>xxv</b>
<b>1. INTRODUCTION</b> .....	<b>1</b>
1.1 Motivation of Thesis .....	2
1.2 Purpose of Thesis .....	3
1.3 Literature Review .....	5
<b>2. FUEL CELL TECHNOLOGY</b> .....	<b>9</b>
2.1 PEM Fuel Cell Structure .....	12
2.2 Alternative for Automotive Powertrain .....	13
2.3 Fuel Cell System Operation .....	15
2.3.1 Flow management .....	15
2.3.2 Thermal management .....	16
2.3.3 Water management .....	16
2.3.4 Power management .....	16
<b>3. FUEL CELL SYSTEM MODELLING AND CONTROL</b> .....	<b>19</b>
3.1 Fuel Cell System Model .....	19
3.1.1 Stack .....	20
3.1.2 Compressor .....	21
3.1.3 Inlet/Outlet manifolds .....	22
3.1.4 Anode flow supplier .....	22
3.1.5 Humidifier .....	23
3.1.6 System efficiency .....	23
3.2 Control System and Architecture .....	24
3.2.1 Control system requirements .....	26
3.2.2 Power controller configuration .....	27
3.2.3 Oxygen excess ratio controller configuration .....	27
3.2.3.1 Reference generator for oxygen excess ratio .....	28
3.2.3.2 Feedforward controller .....	29
3.2.3.3 Feedback controller .....	30
<b>4. SIMULATIONS AND RESULTS</b> .....	<b>31</b>
4.1 Classic PI Controller .....	31
4.2 Fuzzy Logic Based PID Controller .....	33
4.2.1 Fuzzy logic controller .....	34
4.2.2 Setting of scaling coefficients .....	36
4.2.3 Setting of footprint of uncertainty coefficients .....	39
4.3 Comparison of All Controller Configurations .....	41
<b>5. CONCLUSIONS</b> .....	<b>47</b>
<b>REFERENCES</b> .....	<b>51</b>
<b>CURRICULUM VITAE</b> .....	<b>55</b>



## ABBREVIATIONS

<b>An</b>	: Anode
<b>Ca</b>	: Cathode
<b>Cp</b>	: Compressor
<b>FC</b>	: Fuel Cell
<b>FB</b>	: Feedback
<b>FF</b>	: Feedforward
<b>Hm</b>	: Humidifier
<b>IAE</b>	: Integral Absolute Error
<b>LQR</b>	: Linear Quadratic Regulator
<b>MEA</b>	: Membrane Electrolyte Assembly
<b>Membr</b>	: Membrane
<b>OER</b>	: Oxygen Excess Ratio
<b>PEM</b>	: Proton Exchange Membrane
<b>PEMFC</b>	: Proton Exchange Membrane Fuel Cell
<b>PI</b>	: Proportional, Integral
<b>PID</b>	: Proportional, Integral, Derivative
<b>Rm</b>	: Return Manifold
<b>St</b>	: Stack
<b>Sm</b>	: Supply Manifold



## SYMBOLS

<b>A</b>	: Amper
<b>A<sub>T</sub></b>	: Area of Throttle
<b>C<sub>0</sub></b>	: Integral Coefficient of Fuzzy PID Controller
<b>C<sub>e</sub></b>	: Error Normalization Coefficient of Fuzzy PID Controller
<b>C<sub>d</sub></b>	: Error Derivative Normalization Coefficient of Fuzzy PID Controller
<b>C<sub>1</sub></b>	: Proportional Coefficient of Fuzzy PID Controller
<b>e</b>	: Error
<b>η</b>	: Efficiency
<b>H<sub>2</sub></b>	: Hydrogen
<b>I</b>	: Current
<b>φ</b>	: Relative Humidity
<b>K<sub>D</sub></b>	: Derivative Coefficient of PID Controller
<b>K<sub>I</sub></b>	: Integral Coefficient of PID Controller
<b>K<sub>P</sub></b>	: Proportional Coefficient of PID Controller
<b>λ<sub>m</sub></b>	: Membrane Water Content
<b>λ<sub>O<sub>2</sub></sub></b>	: Oxygen Excess Ratio
<b>m</b>	: Mass
<b>O<sub>2</sub></b>	: Oxygen
<b>P</b>	: Power
<b>p</b>	: Pressure
<b>ω</b>	: Rotational Speed
<b>T</b>	: Temperature
<b>u</b>	: Control Input
<b>U</b>	: Energy Density
<b>v</b>	: Vapor
<b>V</b>	: Voltage
<b>W</b>	: Mass Flow Rate
<b>y</b>	: Mole Fraction
<b>z<sub>i</sub></b>	: Lower Degree Membership Value i



## LIST OF TABLES

	<u>Page</u>
<b>Table 2.1</b> : Advantages and disadvantages of various fuel cell types [1]. . . . .	<b>10</b>
<b>Table 3.1</b> : Time constants of various dynamics [2]. . . . .	<b>26</b>
<b>Table 3.2</b> : PI controller tuning result for power controller. . . . .	<b>27</b>
<b>Table 4.1</b> : PI controller tuning result for OER controller. . . . .	<b>32</b>
<b>Table 4.2</b> : Fuzzy logic controller input membership function definition. . . . .	<b>36</b>
<b>Table 4.3</b> : Fuzzy logic controller output membership function definition. . . . .	<b>36</b>
<b>Table 4.4</b> : Fuzzy logic controller rule definition. . . . .	<b>36</b>
<b>Table 4.5</b> : Fuzzy logic controller fuzzy inference setting. . . . .	<b>37</b>
<b>Table 4.6</b> : Fuzzy PID controller tuning result for gain coefficients. . . . .	<b>39</b>
<b>Table 4.7</b> : OER performance statistics for all controller configurations. . . . .	<b>43</b>
<b>Table 4.8</b> : Power performance statistics for all controller configurations. . . . .	<b>45</b>
<b>Table 4.9</b> : Efficiency performance statistics for all controller configurations. . . . .	<b>46</b>



## LIST OF FIGURES

	<u>Page</u>
<b>Figure 1.1</b> : Oxygen excess ratio - net power relation. ....	4
<b>Figure 1.2</b> : Simulation results of fuel cell system under series of step inputs [3].	6
<b>Figure 2.1</b> : Reaction in PEM fuel cell [4]. ....	9
<b>Figure 2.2</b> : Structure of PEM fuel cell [3]. ....	13
<b>Figure 2.3</b> : Schematic of a PEM fuel cell power system [5]. ....	15
<b>Figure 3.1</b> : PEM fuel cell system modelling diagram. ....	20
<b>Figure 3.2</b> : Stack modelling diagram [3]. ....	21
<b>Figure 3.3</b> : Compressor modelling diagram [3]. ....	21
<b>Figure 3.4</b> : Supply manifold modelling diagram [3]. ....	22
<b>Figure 3.5</b> : Return manifold modelling diagram [3]. ....	23
<b>Figure 3.6</b> : Various control configurations for fuel cell system [3]. ....	25
<b>Figure 3.7</b> : Proposed control system architecture for the PEM fuel cell system.	26
<b>Figure 3.8</b> : The maximal power points corresponding to different OER points [6]. ....	28
<b>Figure 3.9</b> : Optimal OER points corresponding to the power request points. ....	29
<b>Figure 4.1</b> : $K_P$ tuning test for classic PI controller, $K_I = 300$ . ....	32
<b>Figure 4.2</b> : $K_I$ tuning test for classic PI controller, $K_P = 30$ . ....	33
<b>Figure 4.3</b> : OER response of the selected configuration of classic PI controller, $K_P=30, K_I=500$ . ....	34
<b>Figure 4.4</b> : Fuzzy logic based PID controller architecture [7]. ....	34
<b>Figure 4.5</b> : Type-1 and Type-2 input membership function definitions [7]. ....	35
<b>Figure 4.6</b> : $C_0$ tuning test for type-1 controller, $C_I = 200$ . ....	37
<b>Figure 4.7</b> : $C_I$ tuning test for type-1 controller, $C_0 = 700$ . ....	38
<b>Figure 4.8</b> : OER response of the selected configuration of fuzzy type-1 PID controller, $C_0 = 700, C_I = 240$ . ....	38
<b>Figure 4.9</b> : $z_1$ tuning test for type-2 controller. ....	39
<b>Figure 4.10</b> : $z_2$ tuning test for type-2 controller. ....	40
<b>Figure 4.11</b> : $z_3$ tuning test for type-2 controller. ....	40
<b>Figure 4.12</b> : $z_4$ tuning test for type-2 controller. ....	41
<b>Figure 4.13</b> : Stack current input for different configurations. ....	42
<b>Figure 4.14</b> : Compressor voltage input for different configurations. ....	42
<b>Figure 4.15</b> : Comparison of OER step responses for several controller configurations. ....	43
<b>Figure 4.16</b> : Comparison of OER responses for classic and fuzzy type-1 feedback controllers. ....	44
<b>Figure 4.17</b> : Comparison of power step responses for several controller configurations. ....	44
<b>Figure 4.18</b> : System efficiency comparison for several controller configurations.	45



## **OPTIMIZED POWER CONTROL STRATEGY FOR A PROTON EXCHANGE MEMBRANE FUEL CELL SYSTEM**

### **SUMMARY**

Global warming has become one of the greatest threats our planet is facing. The primary causes of this threat include the increase in greenhouse gas emissions into the atmosphere as a result of human activities, leading to a strengthening of the greenhouse effect. Factors such as widespread use of fossil fuels, emissions from industrial facilities, agricultural practices, and deforestation contribute to increasing concentrations of greenhouse gases in the atmosphere, causing global warming. To address this issue, increasing the focus on renewable energy sources is of critical importance. Renewable energy sources have the potential to generate energy without harming the environment, thereby reducing greenhouse gas emissions by decreasing the use of fossil fuels. In this context, fuel cell technology presents an innovative approach to clean energy production, offering an effective solution to the problem of global warming.

A fuel cell is an energy conversion device that directly converts chemical energy into electrical energy. This technology typically generates electricity through an electrochemical reaction between hydrogen and oxygen, and also can produce useful outputs such as clean water and heat. Fuel cell technology has a wide range of applications, emerging prominently in both stationary and mobile applications. Stationary use ranges from power generation in power plants to industrial applications, while mobile use extends from transportation vehicles to portable electronic devices. Various types of fuel cells exist, such as solid oxide, alkaline, phosphoric acid, and polymer electrolyte membrane fuel cells. Due to advantages such as high energy density compared to internal combustion engines, high efficiency, and lack of carbon emissions, fuel cell is becoming increasingly prominent in the automotive sector.

The European Union aims to reduce harmful emissions from internal combustion engines with updated emission standards. Additionally, a ban on the sale of gasoline and diesel vehicles is targeted from 2035 onwards, leading to an increase in the importance of electrification in the automotive sector, with rising sales of electric vehicles observed in recent years. Advances in battery technology, incentives, widespread infrastructure, and changing consumer behavior have contributed to the increasing market share of battery electric vehicles. While battery electric vehicles offer advantages such as carbon emissions-free and silent operation, low maintenance costs due to fewer parts, and cheaper charging costs, they also have some disadvantages as a result of relying solely on batteries as the power source. Challenges include long charging times, short battery lifespan, high cost, high weight due to low specific energy

of batteries leading to range limitations, performance degradation in cold weather, and uncontrolled battery fires. In response, the development of hybrid vehicles provides a separate use of the advantages offered by internal combustion engines and batteries, but the long-term effectiveness of this solution is not expected due to the limited lifespan of internal combustion engines. Fuel cell technology presents an alternative solution, potentially replacing internal combustion engines in hybrid vehicles. Fuel cell technology requires a hydrogen-based fuel type and can be stored in a vehicle via hydrogen tanks. As a result, refueling can be done quickly similar to internal combustion engine vehicles, with the only limitation being the size of the tank. With hybrid use, the required battery size decreases, and performance losses can be reduced with efficient energy management. However, fuel cell technology also has some disadvantages that need to be addressed.

One of the main challenges in fuel cell technology is the decrease or deterioration of cell performance due to degradation factors. Catalyst degradation, membrane damage, electrode fouling, water management issues, and voltage losses accelerate cell degradation and reduce its lifespan. Optimizing cell design, selecting suitable electrode materials, using high-quality fuel, and controlling operational conditions considering degradation conditions can extend cell life. From control engineering perspective, improving operational conditions is the main theme of this study. One of the important operational conditions that need to be controlled is oxygen concentration. In situations where oxygen concentration is not controlled, degradation is accelerated. For example, there are studies in the literature showing that oxygen deficiency accelerates degradation. In opposite cases like excess oxygen concentration, there is excessive power consumption due to the overworking of the air compressor. Therefore, oxygen concentration needs to be optimally controlled during power control. This thesis aims to prevent instantaneous drops in oxygen concentration and develop a control strategy that ensures the operation of the cell at optimized oxygen concentration. This control strategy includes power control as well as oxygen concentration control.

The proposed power control strategy is tested on an open-source proton exchange membrane fuel cell system model from Michigan University. This model integrates compressor, supply and return manifold, humidifier, anode flow supplier, and cell stack models. The stack current and compressor voltage are inputs to the system model, while the oxygen excess ratio and net power are outputs of the system model. The control system adjusts system inputs to operate the system at the desired net power and desired settling time and overshoot ratio. While the stack produces power, the power consumption of the compressor is simulated with the applied compressor voltage. The stack model also calculates the oxygen excess ratio by proportioning the oxygen supplied to the consumed. Since the compressor is the dominant power-consuming component, other power-consuming components have been neglected in net power calculations. The anode flow distributor controls fuel supply based on the difference between the supply manifold and anode pressure. The humidifier regulates the operation of the cell stack at the set humidity. Collectors are modeled by assuming a collected volume and used in thermal conduction and fluid dynamics calculations.

Oxygen concentration is controlled through a parameter called the oxygen excess ratio. The ratio of the supplied oxygen to the consumed oxygen during power generation is

given as the oxygen excess ratio. Since the oxygen fed into the system cannot be less than the oxygen used, the value of this ratio can theoretically be a minimum of 1. Since the oxygen fed into the system is proportional to the power consumption of the compressor motor, and the oxygen consumed is proportional to the current drawn, and the current drawn is also proportional to the power generated by the cell. The net power obtained from the fuel cell system is obtained by subtracting the power consumed by the compressor from the power generated from the cell. Although the option of high cell current - low operating voltage for compressor seems suitable for maximizing net power, the desired power cannot be obtained due to inadequate oxygen supply. Therefore, compressor voltage should be regulated to provide optimized oxygen excess ratio to maximize the net power. In this study, a look-up table based reference oxygen excess ratio generator is used via curves of experimental data. The oxygen excess ratio that maximizes the desired power is provided to oxygen excess ratio controller as a reference.

One of the difficulties in controlling the excess oxygen ratio is the disturbance effect of cell current. With increasing cell current, reactions accelerate, requiring an increased amount of oxygen to be used. However, if the compressor voltage is not increased in parallel with the increase in current, the excess oxygen ratio becomes insufficient instantly. This situation is called oxygen starvation and has an accelerating effect on cell degradation. To prevent oxygen starvation, changes in compressor voltage parallel to changes in cell current must be applied. In this study, a current-dependent static feedforward controller is used. A feedforward compressor voltage term is generated in proportion to the applied current, and it is added to the compressor voltage generated by the feedback controller to obtain the final compressor voltage applied to the compressor. Test results have shown that sudden decreases in oxygen level are avoided thanks to the feedforward controller.

The fuel cell power system is a good example of a non-minimum phase system. When the reference oxygen excess ratio is reached, the power is guaranteed to be maximized while improving the transient response of oxygen dynamics leads to a decrease in net power for a moment due to excessive compressor consumption. The classic PI control method has been preferred as the initial configuration for the control of oxygen excess ratio and power. The reason for its frequent preference in industry, its simple mathematical structure and adjustable flexibility with calibration parameters. The fuel cell system exhibits different responses at each operating point due to its complex nonlinear system characteristics. Therefore, rather than analytical methods, tuning of controller parameters is executed experimentally.

Non-minimum phase dynamics result infeasible usage of classical PID controllers due to insufficient stability. To have a better settling time performance for oxygen excess ratio, nonlinear fuzzy logic-based PID controller is proposed as an alternative to linear PI controllers. In the final section, fuzzy type 1 and type 2 PID controllers are tested. While better transient results are obtained after experimental tuning of scaling coefficients for the type-1, no improvement is observed with the adjustment of the type-2 controller. Therefore, the use of a type-1 fuzzy logic-based PID controller has yielded the best results in terms of oxygen transient dynamics. An efficiency formula is derived for this study and implemented within the model. It indicates that system

have an efficiency range of 45-50%. Additionally, optimality of OER brings 0.6% improvement in efficiency compared to a non-optimal scenario.



## PROTON DEĞİŞİM MEMBRANLI YAKIT HÜCRESİ SİSTEMİ İÇİN OPTİMİZE EDİLMİŞ GÜÇ KONTROL STRATEJİSİ

### ÖZET

Küresel ısınma, gezegenimizin karşı karşıya olduğu en büyük tehditlerden biri haline gelmiştir. Bu tehdidin temel nedenleri, insan faaliyetleri sonucu atmosfere salınan sera gazlarının artması ve buna bağlı olarak sera etkisinin güçlenmesidir. Fosil yakıtların yaygın kullanımı, endüstriyel tesislerin emisyonları, artan tarım uygulamalarıyla ormansızlaşma gibi etkenler, atmosferdeki sera gazlarının konsantrasyonlarını artırmakta ve gezegenimizin ısınmasına sebep olmaktadır. Bu sorunun üstesinden gelmek için, yenilenebilir enerji kaynaklarına yönelimin artırılması kritik önem taşır. Yenilenebilir enerji kaynakları, çevreye zarar vermeden enerji üretme potansiyeline sahip olup, fosil yakıtların kullanımını azaltarak sera gazı salınımını düşürmeye yardımcı olur. Bu bağlamda, yakıt hücresi teknolojisi, temiz enerji üretimine yönelik yenilikçi bir yaklaşım sunarak küresel ısınma sorununa etkili bir çözüm sunmaktadır.

Yakıt hücresi, kimyasal enerjiyi doğrudan elektrik enerjisine dönüştüren bir enerji dönüşüm cihazıdır. Bu teknoloji, genellikle hidrojen ve oksijenin elektrokimyasal tepkimeye girmesiyle elektrik üretirken, aynı zamanda temiz su ve ısı gibi faydalı çıktılar da üretebilir. Yakıt hücresi teknolojisi, geniş bir kullanım yelpazesine sahip olup, hem yerleşik hem de mobil uygulamalarda öne çıkmaya başlamıştır. Yerleşik kullanımı elektrik üretimi için güç santrallerinden endüstriyel uygulamalara kadar uzanırken, mobil kullanımı ulaşım araçlarından taşınabilir elektronik cihazlara kadar çeşitlenir. Katı oksit, alkalın, fosforik asit, polimer elektrot membranlı gibi çeşitli yakıt hücresi tipleri bulunur. Konvansiyonel motorlara göre yakıt hücresinin enerji yoğunluğunun fazla olması, yüksek verimi ve karbon emisyonunun olmaması gibi avantajları nedeniyle öne çıkmaya başladığı alanlardan birisi de otomotiv sektörüdür.

Avrupa Birliği, güncellenen emisyon standartlarıyla içten yanmalı motorlardan kaynaklanan zararlı emisyonları azaltmayı hedeflemektedir. Bunun yanı sıra 2035'ten itibaren satılacak tüm otomobillerin sıfır emisyonlu olması dolayısıyla benzinli ve dizel araçların satışının yasaklanmasını hedeflenmektedir. Bu gibi hedefler nedeniyle otomotiv sektöründe elektrifikasyonun önemi artmış ve son yıllarda elektrikli araçların satış rakamlarında yükselme gözlenmiştir. Batarya teknolojisindeki gelişmeler, teşvikler, altyapının yaygınlaşması ve tüketici davranışlarının değişmeye başlamasıyla bataryalı elektrikli araçların pazardaki payı günden güne artmaktadır. Bataryalı elektrikli araçlar karbon emisyonuz ve sessiz sürüş, parça sayısının az olması nedeniyle düşük bakım maliyeti, şarj maliyetinin ucuz olması avantajları sunmasına karşılık tek güç kaynağı olarak batarya kullanması neticesinde bazı dezavantajlara da sahiptir. Gerekli şarj süresinin yüksek olması, bataryanın hızlı tükenen ömrü ve buna karşılık

yüksek maliyeti, bataryaların düşük özgül enerjisi nedeniyle getirdiği yüksek ağırlık ve menzil kısıtlaması, soğuk hava şartları ve hızla orantılı olarak performans kayıpları ve batarya yangınlarının kontrol alınamaması gibi problemler bataryalı araçların yaygınlaşmasını önlemektedir. Buna yönelik olarak hibrit araçların geliştirilmesiyle içten yanmalı motor - batarya birlikteliği sunmuş oldukları avantajların ayrı olarak kullanımını sağlamış olur, ancak içten yanmalı motorların belli bir vadesi olması nedeniyle bu çözümün de uzun vadede etkili olması beklenmemektedir. Yakıt hücresi teknolojisinin, hibrit araçlarda içten yanmalı motorun yerini alması alternatif bir çözümlerden biridir. Yakıt hücresi teknolojisi hidrojen bazlı bir yakıt türü gerektirmektedir, ve hidrojen tankı vasıtasıyla araçta depo edilebilmektedir. Bu haliyle içten yanmalı motorlu araçlara benzer şekilde depo dolumu hızlı bir şekilde yapılabilen ve menzil açısından tek kısıt depo büyüklüğü olmaktadır. Hibrit kullanımla birlikte gerekli batarya boyutu azalmakta ve verimli enerji yönetimiyle beraber performans kayıpları azaltılabilmektedir, ancak yakıt hücresi teknolojisinin de getirmiş olduğu bazı dezavantajlar vardır ve bunların da giderilmesi gerekir.

Yakıt hücresi teknolojisindeki başlıca sıkıntılardan bir tanesi bozunum faktörlerine bağlı olarak hücrenin performansının azalması veya bozulmasıdır. Katalizör zayıflaması, membran hasarı, elektrot kirlenmesi, su yönetimindeki problemler ve voltaj kayıpları yakıt hücresinin bozunumunu hızlandırır ve ömrünü azaltır. Hücre tasarımının optimizasyonu, uygun elektrot malzeme seçimi, yüksek kaliteli yakıt kullanımı ve operasyonel koşulların bozunum koşulları gözetilerek kontrol edilmesiyle hücre ömrü uzatılabilir. Kontrol mühendisliği kapsamında bu çalışmada operasyonel koşullara odaklanıldı. Yakıt hücresi sistemlerinde kontrol edilmesi gereken önemli operasyonel koşullardan bir tanesi oksijen konsantrasyonudur. Oksijen konsantrasyonu, kontrol edilmediği durumlarda bozunumu hızlandırabilir. Örneğin oksijen konsantrasyonu yetersizliğinin bozunumu hızlandırdığını gösteren çalışmalar vardır. Oksijen konsantrasyonu fazlalığı durumundaysa hava kompresörünün fazla çalışması nedeniyle fazla güç tüketimi vardır. Dolayısıyla güç kontrolü sırasında oksijen konsantrasyonunun optimize edilmesi gerekmektedir. Bu tez çalışmasında yakıt hücresindeki değişen çalışma koşullarında oksijen konsantrasyondaki anlık düşmelerin engellenmesi ve optimize edilmiş oksijen konsantrasyonunda hücrenin çalışmasını sağlayacak kontrol stratejisinin geliştirilmesi hedeflenmiştir. Bu kontrol stratejisi oksijen konsantrasyonunun yanı sıra güç kontrolünü de içermektedir.

Önerilen güç kontrol strateji, Michigan Üniversitesine ait açık kaynaklı bir proton değişim membranlı yakıt hücresi sistemi modeli üzerinde yapılan simülasyonlarla geliştirilmiştir. Bu modelde yakıt hücresi sistemi kompresör, besleme ve geri dönüş manifoldu, nemlendirici, anot akış sağlayıcısı ve hücre yığını modellerinin birleştirilmesiyle sistem modeli oluşturulmuştur. Hücre yığını akımı ve kompresör gerilimi sistem modelinin girişleri olup oksijen fazlalık oranı ve net güç sistem modelinin çıktılarıdır. Kontrol sistemi istenilen net güçte sistemi çalıştıracak şekilde sistem girişlerini ayarlar ve sistem çıktıları istenilen oturma süresi ve aşım oranı doğrultusunda kontrol eder. Hücre yığını güç üretirken kompresörün uygulanan gerilimle birlikte güç tüketimi simüle edilir. Hücre yığını modeli aynı zamanda elektrokimyasal denklemler vasıtasıyla beslenen oksijene karşılık uygulanan akıma göre tüketilen oksijeni oranlayarak oksijen fazlalık oranı adında değişkeni hesaplar. Kompresörün baskın güç tüketici komponent olması dolayısıyla diğer güç tüketici

komponentler net güç hesaplamasında ihmal edilmiştir. Anot akış sağlayıcısı sisteme ait olup besleme manifolduyla anot basıncı arasındaki farka göre yakıt beslemesini kontrol eder. Nemlendirici de hücre yığınının ayarlanmış nemde çalışmasını regüle eder. Kolektörler toplanmış hacim varsayımıyla modellenerek ısı iletim ve akışkan dinamikleri hesaplarında kullanılır.

Oksijen konsantrasyonu, literatürde de oksijen fazlalık oranı adı verilen bir parametre vasıtasıyla kontrol edilir. Sisteme beslenen oksijenin kullanılan oksijene oranı oksijen fazlalık oranı olarak verilir. Beslenen oksijen miktarı kullanılan oksijene oranı olarak verilir. Beslenen oksijen miktarı kompresör motorunun tükettiği enerjiyle orantılıyken, kullanılan oksijen miktarı hücreden geçen akımla orantılıdır. Hücreden geçen akım aynı zamanda yakıt hücresinden üretilen güçle orantılıdır. Yakıt hücresi sisteminden elde edilebilecek net güç, kompresör gibi güç tüketen yardımcı komponentlerin çalıştırılmasına harcanan gücün hücreden elde edilen güçten çıkarılmasıyla elde edilir. Net gücü maksimize edebilmek için de yüksek hücre akımı - düşük kompresör gerilimi seçeneği uygun gibi gözükse de yetersiz oksijen beslemesi sonucu istenilen güç elde edilemez. Dolayısıyla kompresör gerilimi, optimize edilmiş oksijen fazlalık oranını verecek şekilde üretilmelidir. Bu çalışmada deneysel eğriler kullanılarak tablo-bazlı güce bağlı olarak referans oksijen fazlalık oranı üreticisi tasarlanmıştır. Çalışılmak istenen güçte maksimum verimi sağlayan oksijen fazlalık oranı kontrol sistemine referans olarak verilmektedir.

Oksijen fazlalık oranı kontrolündeki sıkıntılardan bir tanesi de hücre akımının bozucu etki olarak etki etmesidir. Artan hücre akımıyla birlikte reaksiyonlar hızlanacağından kullanılması gereken oksijen miktarı artması gerekir ancak akımdaki artışa paralel olarak kompresör gerilimi artırılmazsa oksijen fazlalık oranı anlık olarak yetersiz kalır. Bu duruma oksijen açlığı denir ve hücre bozunumunu hızlandırıcı bir etkiye sahiptir. Oksijen açlığının önlenmesi için hücre akımındaki değişime paralel kompresör geriliminde değişimler uygulanmalıdır. Bu çalışmada akıma bağlı statik ileri beslemeli kontrolcü kullanılmıştır. Uygulanan akımla doğru orantılı olarak ileri besleme kompresör gerilimi terimi üretilir, ve geri beslememe kontrolcünün ürettiği kompresör gerilimine eklenerek nihai kompresör gerilimi elde edilir ve kompresöre uygulanır. İleri beslemeli kontrolcü sayesinde oksijen seviyesindeki ani düşmelerin engellendiği test sonuçlarında gösterilmiştir.

Yakıt hücresi güç kontrol sistemi minimum fazlı olmayan sisteme iyi bir örnektir. Referans oksijen fazlalığı oranı yakalandığında güç maksimize edilirken oksijen dinamiklerinin geçici cevabının iyileştirilmesi sırasında kompresör tüketimi fazla olacağından net güçte anlık düşmeye neden olabilir veya istenilen miktarda gücün üretilmemesine neden olabilir. oksijen fazlalığı oranı ve güç kontrolünde kontrolcü tasarımında başlangıç fazında klasik PI kontrol yöntemi tercih edilmiştir. Endüstride de sık olarak tercih edilmesiyle kanıtlanmış performansı, basit bir matematiksel yapıya sahip olması ve kalibrasyon parametreleriyle ayarlanabilir esnekliği dolayısıyla tercih edilmiştir. Yakıt hücresi sistemi kompleks doğrusal olmayan sistem karakteristiği nedeniyle her çalışma noktasında farklı tepkiler vermektedir. Dolayısıyla analitik parametre ayarlama methodları kullanımı yerine kontrolcü parametrelerinin ayarlanması deneysel olarak gerçekleştirilmiştir. Klasik PI kontrolcünün yerleşme

zamanında istenilen performansı vermemesi ve klasik PID'nin stabilite sorunları nedeniyle gelişmiş bir kontrolcü olan bulanık mantık tabanlı PID kontrolör kullanımı önerilmiştir.

Son bölümde gelişmiş kontrolcü yöntemi olarak bulanık tip 1 ve tip 2 PID kontrolcüler denenerek klasik kontrolcüsüyle elde edilen sonuçlarla karşılaştırılmıştır. Ölçeklendirme katsayıları değiştirilerek tip-1 kontrolcü, ve üyelik fonksiyonu belirsizlik ayakizi katsayıları değiştirilerek tip-2 kontrolcüler test edilmiştir. Elde edilen deneysel sonuçlarda tip 1 kontrolcünün ölçeklendirme katsayılarının ayarlanmasıyla klasik PI kontrolcüye göre iyi sonuçlar elde edilse de tip-2 kontrolcünün ayarlanmasıyla sonuçlarda iyileşme görülmemiştir. Dolayısıyla tip-1 bulanık mantıklı PID kontrolcünün kullanılması oksijen dinamikleri açısından en iyi sonucu vermiştir. Önerilen kontrolcü konfigürasyonu yalnız klasik kontrolcü kullanımına göre önemli ölçüde yerleşim zamanını iyileştirmiştir. Verim ifadesi bu çalışma için türetilmiş olup modele entegre edilmiştir. Yakıt hücresi sisteminin test edilen güç noktalarında %45-50 civarlarında verimle çalıştığı gösterilmiştir. Ayrıca oksijen fazlalık oranı kontrolünde optimal oranın sağlanması durumunda sağlanmadığı duruma göre %0.6'lık bir iyileşme sağladığı gösterilmiştir.

## 1. INTRODUCTION

Global warming has become one of the greatest threats our planet facing. The primary causes of this threat include the increase in greenhouse gas emissions into the atmosphere as a result of human activities, leading to a strengthening of the greenhouse effect. Factors such as widespread use of fossil fuels, emissions from industrial facilities, and agricultural-related deforestation contribute to increasing concentrations of greenhouse gases in the atmosphere, causing global warming. To address this issue, increasing focus on renewable energy sources is critically important. Renewable energy sources have the potential to generate energy without harming the environment, thereby reducing greenhouse gas emissions by decreasing the use of fossil fuels. In this context, fuel cell technology presents an innovative approach for clean energy production, and is offering an effective solution to the problem of global warming.

A fuel cell is an energy conversion device that directly converts chemical energy into electrical energy. This technology typically generates electricity through an electrochemical reaction between hydrogen and oxygen, and can also produce useful byproducts such as water and heat. Fuel cell technology has a wide range of applications, emerging prominently in both stationary and mobile applications. Stationary use ranges from power generation in power plants to industrial applications, while mobile use extends from transportation vehicles to portable electronic devices. Various types of fuel cell exist, such as solid oxide, alkaline, phosphoric acid, molten carbonate and proton exchange membrane fuel cells. Due to advantages such as high energy density compared to conventional motors, high efficiency, and lack of carbon emissions, hydrogen-based technology is becoming increasingly prominent in the automotive sector.

The European Union aims to reduce harmful emissions from internal combustion engines with updated emission standards. Additionally, a ban on the sale of gasoline

and diesel vehicles is targeted from 2035 onwards, leading to an increase in the importance of electrification in the automotive sector, with rising sales of electric vehicles observed in recent years. Advances in battery technology, incentives, widespread infrastructure, and changing consumer behavior have contributed to the increasing market share of battery electric vehicles. While battery electric vehicles offer advantages such as carbon emissions-free and silent operation, low maintenance costs due to fewer parts, and cheaper charging costs, they also have some drawbacks as a result of relying solely on batteries as the power source. Challenges include long charging times, short battery lifespan, high cost, high weight due to low specific energy of batteries leading to range limitations, performance degradation in cold weather, and uncontrolled battery fires. Alternatively, development of hybrid vehicles provides a separate use of both advantages offered by internal combustion engines and batteries, but long-term effectiveness of this solution is not expected due to the limited lifespan of internal combustion engines. Fuel cell technology presents an alternative solution, potentially replacing internal combustion engines in hybrid vehicles. Fuel cell technology requires fuel as hydrogen which can be stored in a vehicle via hydrogen tanks. As a result, refueling can be done quickly similar to internal combustion engine vehicles. The only factor limiting the range of the vehicle is the volumetric capacity required by vehicle to store hydrogen tanks. With hybrid use, the required battery size decreases, and performance losses can be minimized with efficient energy management. However, fuel cell technology also has some downsides that need to be addressed.

## **1.1 Motivation of Thesis**

One of the main challenges in fuel cell technology is deterioration of cell performance due to degradation factors. Catalyst degradation, membrane damage, electrode poisoning, water management issues, and voltage losses accelerate cell degradation and reduce lifespan. Optimizing cell design, selecting suitable electrode materials, using high-quality fuel, and controlling operational conditions that considering degradation conditions can extend cell life. This study addresses issues pertaining to control engineering. One of the significant operational conditions that need to be

controlled is oxygen concentration. In situations where oxygen concentration is not controlled, degradation is accelerated. For example, there are studies in the literature showing that oxygen deficiency accelerates degradation [8]–[10]. In cases of excess oxygen concentration, there is excessive power consumption due to the overworking of the air compressor. Therefore, oxygen concentration needs to be optimally controlled during power control. This thesis aims to prevent instantaneous drops in oxygen concentration and develop a power control strategy that ensures the operation of the cell at optimized oxygen concentration.

## **1.2 Purpose of Thesis**

This study proposes an optimized power control strategy aiming maximal efficiency for fuel cell systems used in automobile propulsion units. In automotive applications, a fuel cell controller communicates with a vehicle control unit to determine power demand. To generate necessary power, the fuel cell controller determines the stack operating current and ensures generation of required electrical voltage at this operating current. A fuel cell stack serves as the primary power generator, in contrast components such as compressor, pump, heater, and humidifier are consumer. Compressor accounts for significant portion of the consumed power; therefore, its performance is critical for power dynamics. Even in a modelling study [11], net power generated by a fuel cell system is obtained by subtracting compressor power from power generated by the stack, via neglecting other auxiliary power consumers. Efficiency of fuel cell can be increased by producing highest power from the supplied chemical energy of fuel per time, with also minimizing the losses. Optimal usage of the compressor has significant contributions to power efficiency. However, excessively low power consumption of the compressor adversely affects cell performance. The compressor supplying inadequate amount of oxygen to the stack results in oxygen starvation, and leads to permanent performance deterioration of fuel cell stack. Therefore, it is necessary to operate compressor optimally to ensure maximum efficiency without loss in stack power and protect against oxygen starvation phenomenon for preserving stack lifespan. Hence, oxygen concentration is very critical for fuel cell system during a power control application. Oxygen

concentration is regulated by a parameter known as the oxygen excess ratio(OER) in the literature [3,6,12,13]. OER is defined as ratio of supplied oxygen to the oxygen consumed within stack. Since the oxygen supplied into the system cannot be less than the oxygen consumed, theoretically, minimum value of this ratio can be 1. Relationship between OER and net power performance is presented, as shown in Fig. 1.1. According to figure, OER seems not have a significant effect on net power under low power demands; however, it has a notable impact on net power under high power demands. For instance, at a working current of 280 A, an excess ratio of 1.5 results in approximately 45 kW power generation, whereas an excess ratio of 2 leads to nearly 52 kW power generation. Therefore, sustaining the optimal OER results in maximal power generation. In this study, a reference OER generator is derived using data-based methods, and utilized for OER control.

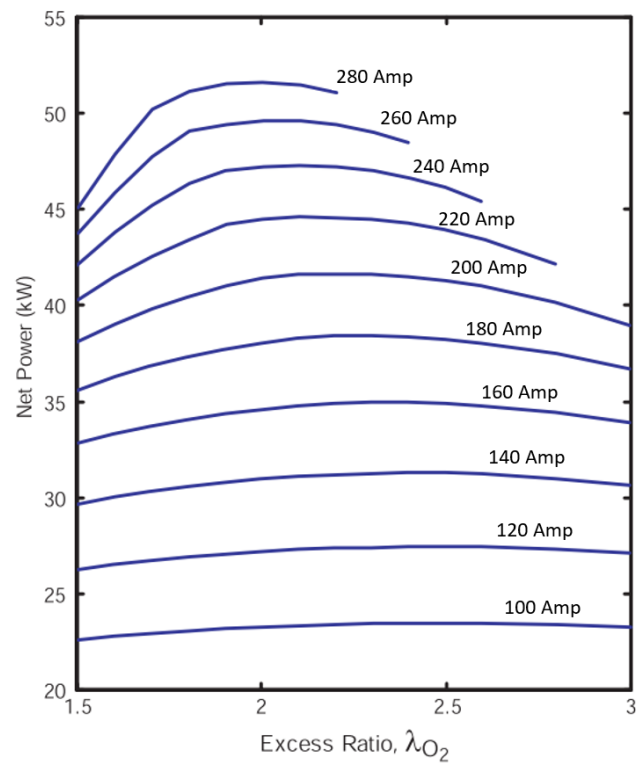


**Figure 1.1 :** Oxygen excess ratio - net power relation.

Another challenge in power control is the mutual disturbance effect between the oxygen excess ratio and net power. For example, when the operating current is increased to achieve a higher power, there will be a instant increase in oxygen consumption, leading to a significant decrease in OER due to supply insufficiency. This

effect can be observed at the 2, 6 and 14th seconds in Fig. 1.2 (e). This situation causes instantaneous oxygen starvation phenomenon, reducing the lifespan of the cell as a degradation effect with each cycle. As a second example, if the stack current remains constant but OER is increased with higher compressor voltage at 18th second, seen in Fig. 1.2 (d), instant power drop is observed. To prevent sudden drops in net power and excess ratio, a feedforward controller is utilized to produce additional compressor voltage based on the operating current. Feedforward controller adds compressor voltage parallel to changes in the operating current, which prevents insufficiency of OER against power transitions.

For OER control, it is essential to use a feedback controller in addition to the feedforward controller, because under possible disturbances, the controller can erroneously set OER to a non-optimal value. Therefore, in this study, a feedforward plus feedback structure is proposed for excess ratio control. Due to complex nonlinear dynamics of the PEM fuel cell model [11], a more advanced type of controller, namely fuzzy-logic PID controller, has been employed. Type-1 and type-2 fuzzy controllers, which offer greater degrees of freedom, have been tested to improve the transient system response and results are compared with the classical PID controller. An efficiency formula is derived and implemented within model to show the system overall efficiency, and proposed methods performance in efficiency increase.

### **1.3 Literature Review**

The 1990s and 2000s were when many automotive manufacturers intensified their research and development efforts on fuel cell vehicles. During this time, particularly Japanese automakers such as Toyota, Honda, and Nissan, European brands like Daimler Chrysler and Volkswagen, and American automakers like Ford prioritized their work on fuel cell vehicles. Some prototype models and concept vehicles were also produced during this period. Ford's fuel cell system developed for passenger cars [5] served as reference data for the research conducted by Pukrushpan and colleagues at Michigan for their doctoral studies [3], and enables development of an open-source realistic fuel cell system model [11]. This provided opportunities for advancement of fuel cell systems in commercial use and capabilities of testing advanced controllers

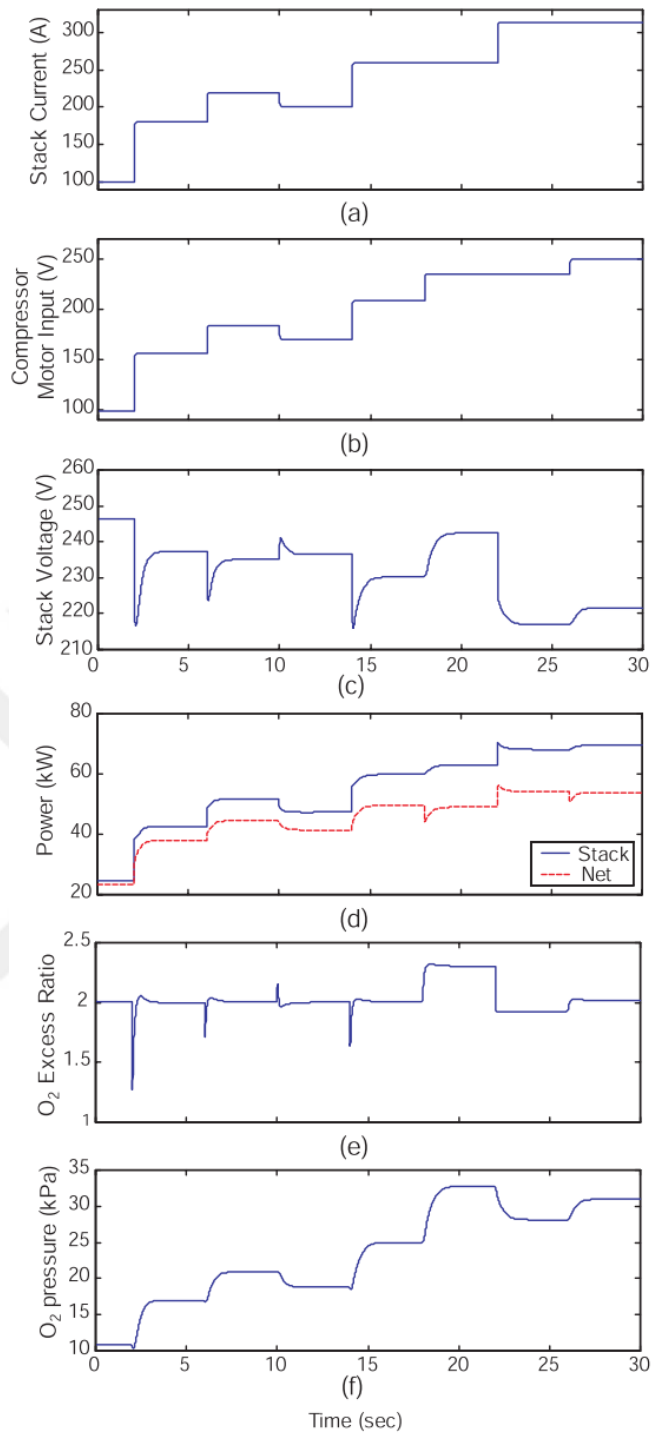


**Figure 1.2 :** Simulation results of fuel cell system under series of step inputs [3].

in an academic context. The model is utilized in this thesis for testing purposes and is examined in Chapter 3. Due to the dominant dynamics of the air supply system in PEM fuel cells, control-related efforts have generally been focused on air path. Therefore, the studies in literature focusing air control are examined. Pukrushpan [3]

also presents a model-based control design for the air supply, specifically the OER. Linear quadratic regulator (LQR) based state feedback controller is accompanied by a dynamic feedforward controller. It is compared with a classical PI controller. The state feedback controller gives better results for the OER transients especially in terms of robustness; therefore, it is proposed. Kendir [6]'s study focuses on maximizing the net power via utilizing a fuzzy logic reference generator and fuzzy feedforward controller accompanied by a classical PI controller. He uses fuzzy logic inference to handle dominant nonlinearity and a reference generator to maximize net power against various stack currents. Yin [12] uses a classical PID controller and neural network based tuning algorithm to get better transients for the OER. Ma [14] introduces a reduced order control technique that rejects disturbances actively, designed for air intake system of PEMFC, utilizing the estimation of the OER. In this study, the assumptions that OER is not measurable with a sensor but needs to be estimated by utilizing a reduced-order extended state observer.

None of the studies mentioned is interested in power management. The power management system is responsible for generating power according to demand from the vehicle control unit. During power generation by the stack, losses also occur through auxiliary components. In this study, a net power control strategy is proposed to maximize the system's efficiency. The OER plays a crucial role in system efficiency and its transient in stack lifespan. The previous studies were interested in obtaining better OER transients against stack current step inputs. However, it is possible to observe different transient dynamics other than step-wise in the current during power transitions. Neglecting power dynamics could cause the load current to be perceived as a disturbance for the OER control, as seen in Fig. 1.2 (e). Therefore, power dynamics must be considered during OER control, and sudden drops in OER due to power transitions shall be avoided. At first, a classical PI controller is adapted to control net power, obtaining stack current as controller output. A static feedforward controller is implemented to compensate for the disturbance effect of power dynamics into the OER. The same transients of stack current are added to the compressor voltage with a gain and an offset. The optimal OER that maximizes the net power is targeted via a reference generator, as in [6]. Due to transients of stack

current, it is not desired that reference OER is continuously changing. Therefore, the structure is changed, and current-based reference generator is transformed into a power demand-based one. The reference generator is designed as a look-up table. PI controller typically used in OER feedback, is replaced with a more advanced controller type called fuzzy PID controller structure to handle dominant nonlinearity. Finally, the different controller configurations for OER, including feedforward controller, classical feedback controller, feedforward plus classical, and feedforward plus fuzzy feedback controllers, are compared. Overall efficiency of the fuel system model and the efficiency improvement with optimal OER usage is presented.

Chapter 2 introduces fuel cell technology fundamentals. Thereafter, it focuses system interactions that need to be controlled, when fuel cell technology is used as a propulsion system in automobiles. In Chapter 3, a PEM fuel cell system model is reviewed. The proposed control strategy is tested on this model. Following, the requirements and details regarding the designed control system are discussed. Chapter 4 introduces different types of controllers that can be used in feedback control, and tuning results. Finally, the effects of different control configurations are compared regarding OER, power, and efficiency results. Chapter 5 summarizes proposed studies, analyses the results, and presents future possible improvements to this study.

## 2. FUEL CELL TECHNOLOGY

Fuel cell principles were discovered by Sir William Grove [15]. He invented a voltaic cell that generates electricity through the reaction of hydrogen and oxygen. An electrolyte between two electrodes, namely anode and cathode allows the flow of positive ions while electrons flow through a circuit from anode to cathode, and results with a potential voltage difference (2.1). Water is produced in cathode after positive ions which is  $H^+$  reaction with oxygen molecules (2.2). The reaction is illustrated in Fig. 2.1.

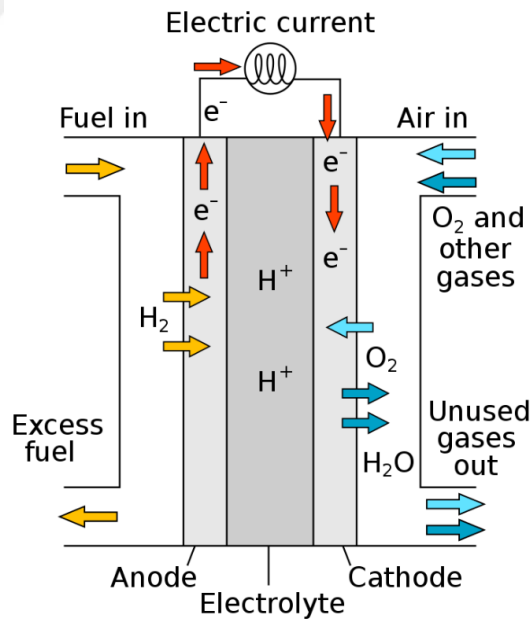


**Figure 2.1 :** Reaction in PEM fuel cell [4].

Francis Thomas Bacon pioneers the commercialization of this technology [16]. In the following years, it became part of significant projects as a power source, for

instance NASA Apollo space missions. The structure of fuel cell inherently emits heat, making it also highly useful for heating applications in addition to electricity generation [17]. Depending on the application, the type of fuel and oxidant used, the electrolyte type, and operating temperature, has been changing. Several type of fuel cells are summarized in table 2.1. Due to its high efficiency and zero or low carbon emissions, this technology is emerging as an alternative for fossil fuel based power sources. Transportation is one of the promising sector that fuel cell technology is utilized as a substitution to internal combustion engines. Recent studies reveal that carbon dioxide ( $CO_2$ ) constitutes over 97% of greenhouse gas emissions, with the transportation sector alone responsible for 38% of  $CO_2$  emissions [18]. Fuel cell technology is therefore important to reduce these emission rates. In this paper, fuel cell technology is focused as a powertrain tool for automobiles. Proton Exchange Membrane(PEM) is the most suitable fuel cell type due to its high energy density, high durability with offering low temperature operating conditions. This chapter presents the conditions to be considered for the utilization of PEM fuel cells as automotive power units from the perspective of control engineering.

**Table 2.1 :** Advantages and disadvantages of various fuel cell types [1].

Fuel Cell Type	Advantage	Disadvantage
Polymer electrolyte membrane fuel cell (PEMFC)	<ul style="list-style-type: none"> <li>• High energy density</li> <li>• Suitability for both mobile and stationary usage</li> <li>• Low temperature operation (80°C)</li> <li>• Quick startup</li> <li>• Less wear</li> <li>• High durability</li> <li>• Low weight and volume</li> </ul>	<ul style="list-style-type: none"> <li>• Expensive catalyst</li> <li>• Susceptible to poisoning by carbon monoxide (CO)</li> </ul>

**Table 2.1 (continued) :** Advantages and disadvantages of various fuel cell types [1].

Fuel Cell Type	Advantage	Disadvantage
Direct methanol fuel cell (DMFC)	<ul style="list-style-type: none"><li>• Usage of methanol as a fuel</li><li>• Easier storage with higher energy density</li><li>• Easier to transport and supply fuel</li><li>• Suitable for portable applications</li></ul>	<ul style="list-style-type: none"><li>• Lower power range of applicability</li></ul>
Alkaline fuel cell (AFC)	<ul style="list-style-type: none"><li>• Efficiency up to 60% in space applications</li></ul>	<ul style="list-style-type: none"><li>• Susceptible to poisoning by carbon dioxide (CO<sub>2</sub>)</li><li>• Lower power range of applicability</li><li>• Operation at higher temperature</li><li>• Less durability</li></ul>
Phosphoric acid fuel cell (PAFC)	<ul style="list-style-type: none"><li>• Tolerance to impurities in fuel and poisoning</li><li>• 85% efficiency when used for co-generation</li></ul>	<ul style="list-style-type: none"><li>• Higher power range of applicability</li><li>• Less efficiency only in generating electricity (37-42%)</li><li>• Large and heavy</li></ul>

**Table 2.1 (continued) :** Advantages and disadvantages of various fuel cell types [1].

Fuel Cell Type	Advantage	Disadvantage
Molten carbonate fuel cell (MCFC)	<ul style="list-style-type: none"><li>• Coupled-usage with natural gas and coal-based power plants</li><li>• 85% efficiency when used for co-generation</li><li>• Non-expensive metals can be used as catalysts</li><li>• Internal reforming by itself due to high temperature</li></ul>	<ul style="list-style-type: none"><li>• Operation at higher temperature</li><li>• Less durability</li><li>• Higher corrosion</li></ul>
Solid oxide fuel cell (SOFC)	<ul style="list-style-type: none"><li>• Tolerance to impurities in fuel and poisoning</li><li>• 85% efficiency when used for co-generation</li><li>• Non-expensive metals can be used as catalysts</li><li>• Internal reforming by itself due to high temperature</li></ul>	<ul style="list-style-type: none"><li>• Operation at higher temperature (1000°C)</li><li>• Slow startup</li><li>• Requires significant thermal shielding</li><li>• Limited to stationary applications</li></ul>

## 2.1 PEM Fuel Cell Structure

Polymer Electrolyte Membrane or Proton Exchange Fuel Cells (PEMFCs) are the most preferred fuel cells because of their solid electrolyte, extended lifespan, low wear, and high energy density. Due to operating in lower temperature range which is 50–100°C, PEMFCs provide safer a operation and do not require insulation from heat. The PEM, which is both a good conductor of hydrogen ions and an electrical insulator, is usually made of a fluorocarbon. The protons ( $H^+$ ) mobility is increased with membrane hydration. Membrane electrolyte assembly(MEA) places membrane between a pair

of electrodes (cathode and anode) made of highly conductive substances such porous graphite, as depicted in Fig. 2.2.

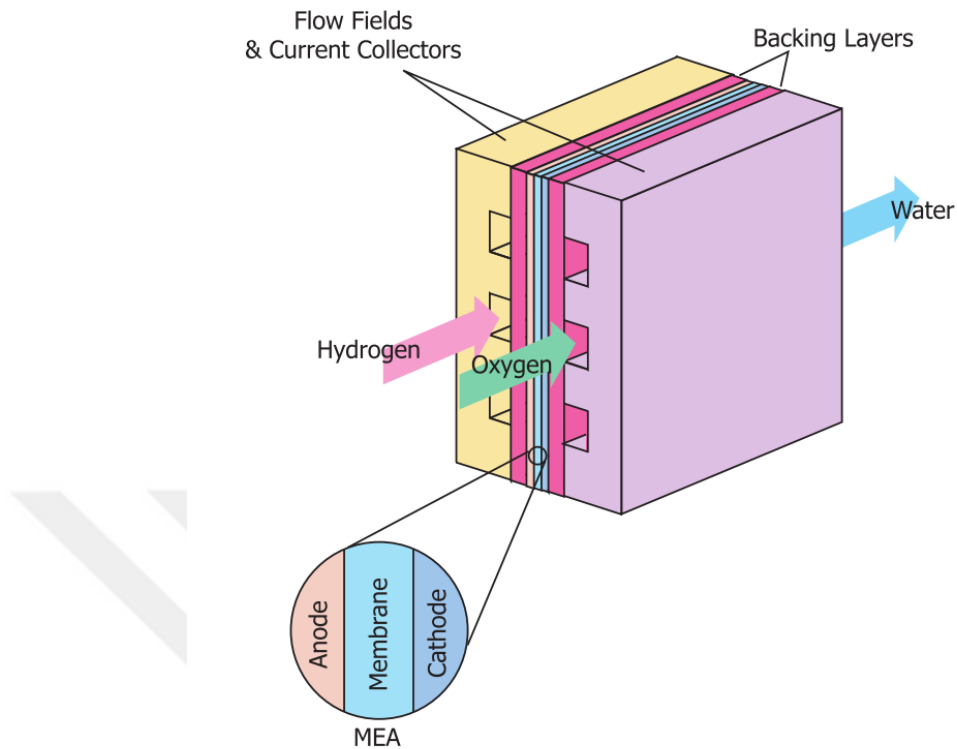


**Figure 2.2 :** Structure of PEM fuel cell [3].

Two carbon-based permeable backing layers encircle the membrane electrolyte assembly. Adequate propagation of streams to the catalyzer on the membrane electrolyte assembly is ensured by the permeable backing layers. The backing layers exterior consists of flow fields, which act as a current collector. A light yet rigid leak-proof substance that transmits electrons is used to make the exterior. The subsequent cell is connected with the opposite side to the exterior. Finally the power demand from the fuel cell system determines how many cells can be placed in a stack.

## 2.2 Alternative for Automotive Powertrain

In recent years, fuel cell systems step forward due to their capability of generating power without carbon emission and high efficiency range, 40 to 60% [19]. On the other hand, internal combustion engines(ICE) are only limited with 30-40% efficiency due to thermal energy conversion. Carnot cycle prevents ICEs to exceed these range [20]. With byproducts of water and heat during power generation, there is no harmful outputs

created for the environment. Similar to batteries, cell generates electrical voltage to impulse electrical powertrain of a car. Compared to battery, charging mechanism of the fuel cell power system differs. Battery store the energy in chemical potential in the cell, while fuel cell systems needs a storage of the fuel generally in gaseous or liquid format. To increase the stored energy, battery itself has to enlarge itself, in contrary fuel cell only has to scale its fuel tanks. From the energy density perspective, fuel cell is superior than battery. This issue brings an advantage for fuel cell to increase the vehicle range only via increasing the size of tanks without adding extra weight as well as in the battery. Moreover, charging process of a battery requires still long time. Fuel cells offer quick refueling process via storing hydrogen similar to ICE cars.

For a fuel cell system to be utilised for vehicle propulsion, it must consist of numerous subsystems. A fuel cell engine's essential parts are displayed in Fig. 2.3. The fuel cell system needs several management. At first, the regulation of reactants is necessary. According to the power request, the sufficient amount of fuel and oxidant needs to be supplied. The fuel is supplied from a hydrogen tank and the oxidant is obtained via pressured air. During reaction, hydrogen molecules transforms into hydrogen ions and flow through the electrolyte. To easier the flow of ions, membrane needs to be humidified. The water is supplied to the membrane via humidified reactant flows. The supplied water is also deionized to prevent reaction with hydrogen ions. Moreover, the water is used to regulate the the temperature of the stack. After reactions, heat is produced and it increases the temperature of the stack. To prevent stack from high temperatures, water is also directly supplied the stack for the cooler effect. As it is mentioned, there are lots of auxiliary components and control of these components required to operate fuel cell system. This complexity of the management is one of the drawbacks of the fuel cell systems. If the system lacks of a proper management, the cell performance will deteriorate, and lifespan of the cell will reduce. The phenomena called degradation is one of the trend topic for fuel cell area. To understand the conditions causing degradation and developing mitigation strategies is the main purpose of these studies. Optimizing operating conditions plays significant role as much as corrosion-resistant and durable material development. Therefore, this paper

focuses on one of the operational condition of fuel cell. The next section overviews fuel cell operational condition regarding the system in Fig. 2.3.

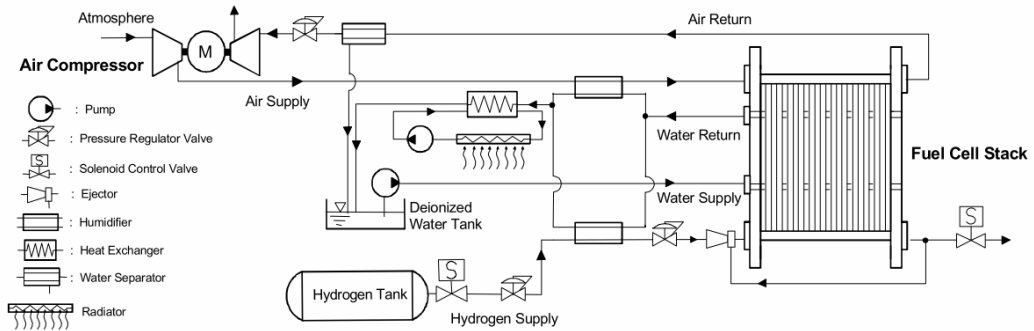


**Figure 2.3 :** Schematic of a PEM fuel cell power system [5].

## 2.3 Fuel Cell System Operation

As mentioned in the previous section, there are several managements that affects fuel cell performance. Continuous observation and control of the system parameters like pressure, temperature, humidity, voltage etc. is necessary to prevent the cell degradation. The fuel cell subsystems can be categorized into 4 group. It is important to notice that each subsystem has relationship with each other. Therefore, it makes it difficult to control of one subsystem independently. The four subsystems are detailed in the following sections.

### 2.3.1 Flow management

The flow management is responsible to ensure sufficient flow rate of reactants, which are hydrogen and oxygen. Hydrogen is supplied via valve to allow hydrogen passage from tanks to fuel cell. Oxygen is supplied via an air compressor. The flow rates are determined according power demands, but there are other properties need to be considered for these flows. The pressure, temperature and humidity of the flows are important for the cell health. For instance, for a overheated flow after exiting from compressor needs to be cooled. For an insufficient thermal management requires the drop of flow rate oxidant to protect stack from overheat.

### **2.3.2 Thermal management**

Thermal management is responsible to sustain stack and system in acceptable temperature range. For the stack, optimal operational temperature is 80°C. The stack is cooled with directly supplying of deionized water and cooled flow of reactants. The temperature control of fuel cell is more challenging than the ICEs, because the temperature difference is relatively low, and deionized water is not as effective as the coolants in the ICE cooling systems. To supply water into stack, pump is used. Heat exchanger is used cool the supplied flows to the stack via transferring heat from them to the cooling water. Also, a cooling fan is used to cool the system. It is important to choose the adequate components and control the system to protect cell from degradation.

### **2.3.3 Water management**

The water management system is responsible for ensuring adequate hydration of the polymer membrane and regulating water distribution within the stack. The water makes easier transition of protons in electrolyte. However inadequate amount of water restrict the passage. The drought, or flooded conditions correspond to water amount is insufficient and excessive. Inadequate humidification control can result in significant voltage reduce, up to 40% [21]. It is important to balance of water in the cell. There shouldn't be too much difference in humidity between cathode and anode. Concentration gradient results with transition of water from one electrode to the another. The water is produced within cathode. It may increase the concentration, and can disrupt to balance. There is a recirculation system is designed that water inside the stack is collected in a tank after its usage as humidifier for flows and cooler flow in heat exchanger.

### **2.3.4 Power management**

The power management is responsible to generate the power demanded. The necessary power is controlled via current flow through stack. The power is generated by stack, on the other hand there are power consumer components such as compressor, pump,

valves etc. It is important to generate power in an efficient way. The compressor is responsible of the major power consumption. The power performance is really affected by the relationship between stack and compressor. For instance, for the lower load current, the efficiency of the system is relatively good because stack does not necessitate much oxygen due to low power demand. Consecutively, compressor does not consume much power. When load current is increase, the power demand is increased. However, the power consumption of the compressor exponentially increase with the increasing current which results with lesser efficiency. Therefore, it is important execute the compressor in the minimum operating voltage that is sufficient to supply oxygen and enables to generate necessary power by stack. In the following chapter, this problem is detailed and proposed control strategy is presented.





### **3. FUEL CELL SYSTEM MODELLING AND CONTROL**

This study proposes a power control strategy based on optimizing oxygen excess ratio response. The study is conducted on the PEM fuel cell model from the University of Michigan library [11]. The control-oriented model was developed within Matlab-Simulink environment. Therefore, the proposed controller is developed in the same environment. This section starts with the introduction of the fuel cell model. Due to the extensive and complex structure of the model, and since modeling is not the primary focus of this thesis, sharing of all equations has been avoided. The efficiency term is derived and implemented within the model. Since the modelling is not the main focus of this study, the model is attempted to be explained solely by block diagrams, and the variables related to efficiency are presented with equations.

#### **3.1 Fuel Cell System Model**

The fuel cell system model is developed based on FORD's P2000 prototype fuel cell electric vehicle [5]. The fuel cell power unit is able to generate 67 kW net power. The fuel cell consists of 3 stacks and 381 cells. Maximum operation temperature is 85°C and stack pressure is 2.07 bar. However, during this study, testing of extreme points are avoided. The system is considered to be operated at moderate operational conditions. In the model, stack is assumed to be operated at a constant temperature, 85°C. This brings advantage of consuming no effort for thermal management. A static humidifier is utilized to set easily the desired humidity at stack. Moreover, a flow proportional controller is utilized instead of pressurized hydrogen tank and control valves to make fuel path more simplified. The dynamics related power electronics also neglected. The main focus of this study is to optimize fuel cell system performance via improving air path control. Therefore the model mainly interested with air path dynamics is selected to test the control strategy proposed by this study.



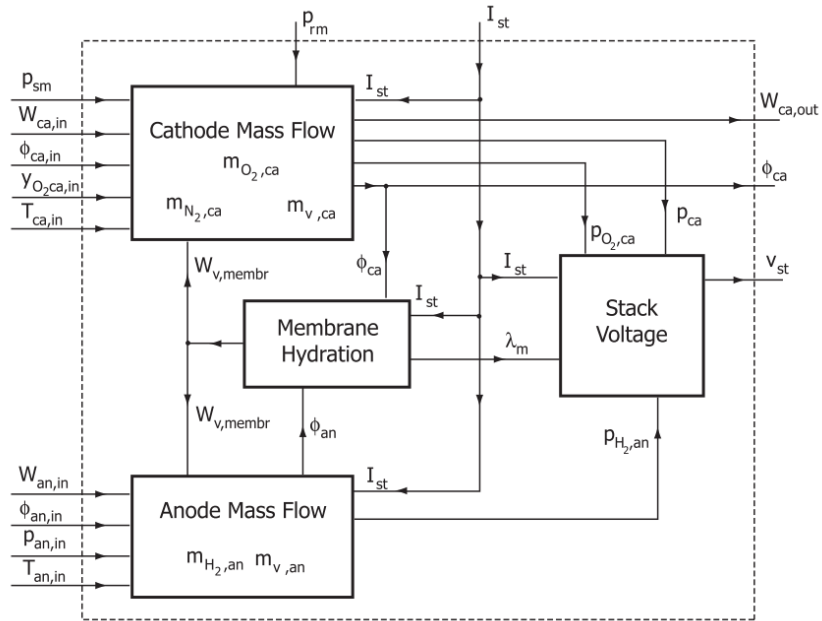


**Figure 3.2** : Stack modelling diagram [3].

### 3.1.2 Compressor

The compressor model is separated into two parts, as shown in Fig. 3.3. The first part is a static compressor map determining the air flow rate through the compressor. Polynomial equations derived from the compressor map is used to calculate the exit air temperature and the power consumed by the compressor ( $P_{CP}$ ). The second part represents the compressor electromechanical dynamics, and calculates the compressor

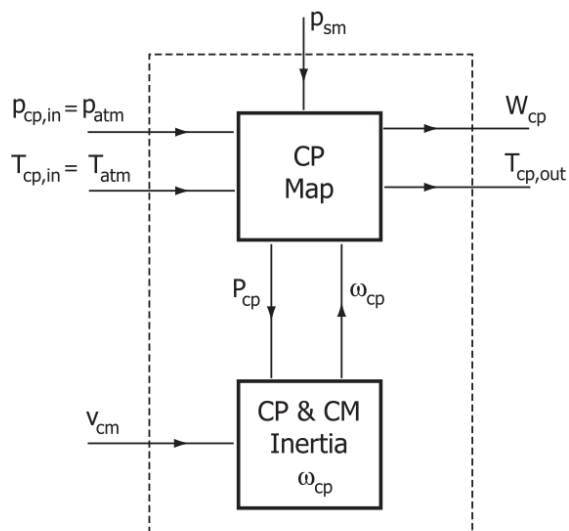


**Figure 3.3** : Compressor modelling diagram [3].

speed regarding compressor efficiency and electrical equivalent circuit approach. The compressor map meanwhile uses the compressor speed to find the air mass flow rate.

### 3.1.3 Inlet/Outlet manifolds

The manifold model with a lumped volume assumption is associated with pipes and connections between each component. Thermal and fluidity properties are considered in calculations. The supply manifold volume includes the volume of the pipes between the compressor and the fuel cell stack including the volume of the cooler and the humidifier. The block diagram of the supply manifold is shown in Fig. 3.4.

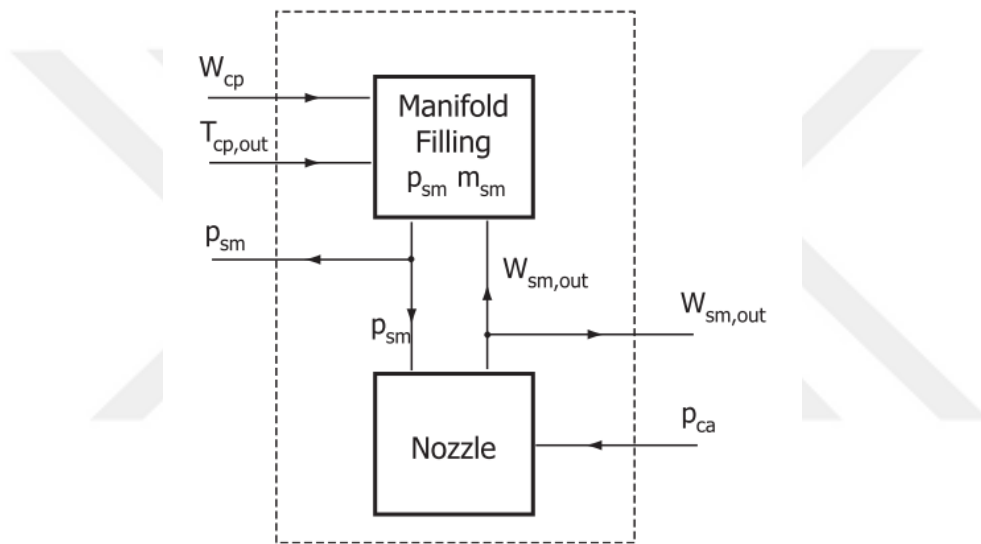


**Figure 3.4 :** Supply manifold modelling diagram [3].

The return manifold represents the pipeline at the fuel cell stack exhaust. The block diagram of the return manifold is shown in Fig. 3.5.

### 3.1.4 Anode flow supplier

As in real life, hydrogen is supplied to the anode of the fuel cell stack by a hydrogen tank. It is assumed that a valve can instantaneously adjust the anode inlet flow rate to maintain the minimum pressure difference between the cathode and the anode. The anode channel flow resistance is small compared to the cathode flow resistance, therefore maintaining the pressure difference ensures sufficient flow of hydrogen for

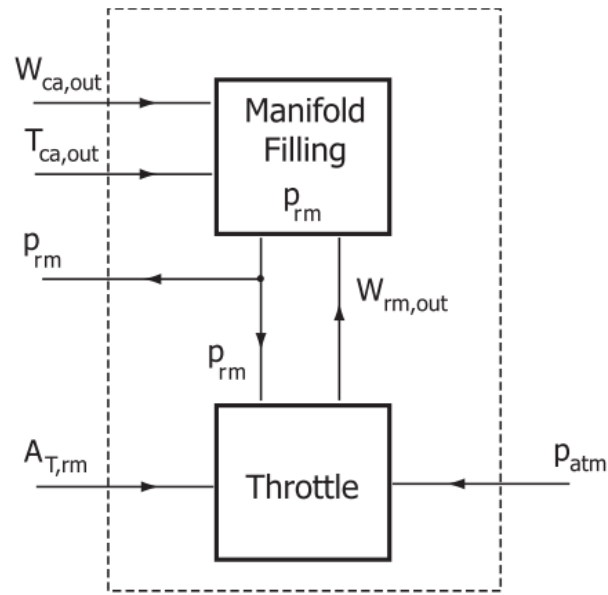


**Figure 3.5 :** Return manifold modelling diagram [3].

the fuel cell reaction. The temperature of the flow is assumed to be equal to the stack temperature. It is also assumed that the conditions of pressure, temperature and humidity, of the anode outlet flow is the same as the condition of the gas in the anode flow channel. Additionally, the flow channel and the backing layer of all cells are lumped into one volume.

### 3.1.5 Humidifier

Air flow from the supply manifold is humidified before entering the stack by injecting water into the air stream in the humidifier. The humidifier's volume is small, and hence, it can be considered part of the supply manifold volume. A static model of the humidifier is used to calculate the change in air humidity due to the additional injected water. For the anode side, fully humidified fuel flow assumption is made, therefore humidifier is only used for the cathode channel.

### 3.1.6 System efficiency

The fuel cell system efficiency formula (3.2) is derived by using internal parameters of the model. System efficiency ( $\eta_{System}$ ) is calculated by dividing generated net power

to the chemical energy of the supplied fuel per time. The hydrogen, the supplied fuel, has an energy density of 120 MJ/kg [22]. Multiplication of energy density( $U$ ) with the flow rate of inlet hydrogen( $W_{H_2,in}$ ) gives the supplied chemical energy per time. The net generated power( $P_{Net}$ ) is calculated by subtracting power consumption of compressor( $P_{Cp}$ ) from power generated by stack( $P_{St}$ ).

$$\eta_{System} = \frac{P_{St} - P_{Cp}}{U \cdot W_{H_2,in}} \quad (3.2)$$

### 3.2 Control System and Architecture

The proposed control system is developed from thesis of Pukrushpan [3]. He proposed 3 different control configurations, seen in Fig. 3.6. In Figure, w, u, y, and z correspond to stack current, compressor voltage, performance variables, and measurements. In his study, OER and net power are included in performance variables(y). These are estimated with an observer using measurement variables(z) and the results are analyzed according to performance variables. In this study, it is assumed performance variables are directly measurable. The current(w) directly acts as a disturbance to the OER performance. Therefore, a current-based feedforward controller is utilized to prevent deviations from the nominal working condition for OER, and generates compressor voltage in 3 configurations. Feedforward controller was designed to set OER to 2 as nominal condition against various load current points. Static and dynamic feedforward controller configurations are designed to set OER to 2 against all current variations in (a) and (b). Further to achieve zero error at steady state and increase the robustness, feedback control is implemented in addition to feedforward in the (c) configuration. However, none of this configurations are ideal because of two reasons. Firstly, setting OER to 2 may give satisfactory results in higher power demands, but it gets far away from the top efficient point when the power demand decreases, as seen in Fig. 3.8. Secondly, instant OER drops are observed during step wise stack current transitions, seen at 2, 6 and 14th seconds in Fig. 1.2(e). This originates from supplied oxygen amount remaining insufficient for the moment consumed oxygen increasing parallel to the stack current. Insufficiency of oxygen is described as oxygen starvation, which as an accelerating phenomena of cell degradation. To prevent starvation, stack current

transitions are smoothed via including power feedback control structure. After, a reference generator is added to catch optimized OER. Feedback controller structure is therefore changed to set OER to the reference value rather than constant 2. The static feedforward controller is utilized to obtain a fast response. The control system performance is measured with a specific requirement determined according to the limits on system dynamics.

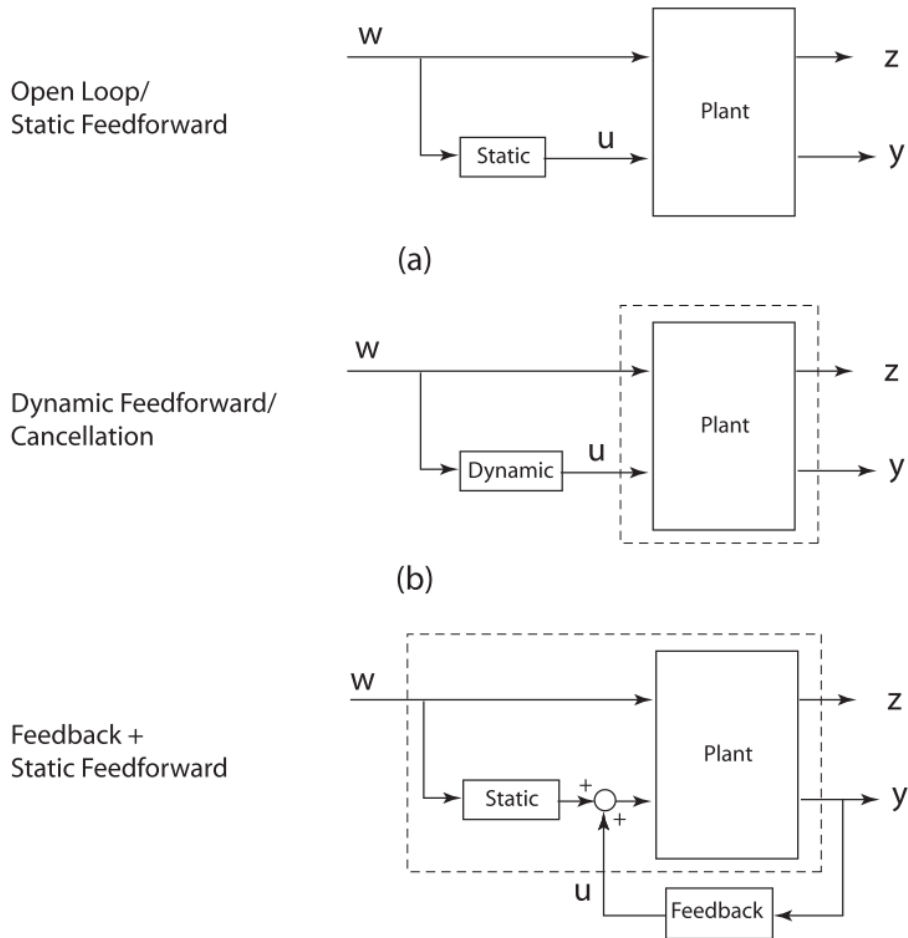


**Figure 3.6 :** Various control configurations for fuel cell system [3].

The proposed control system of the fuel cell system comprises 2 inputs and 2 outputs, as can be seen in Fig. 3.7. Stack current ( $I_{St}$ ) as a first input is used to regulate the net power generated from fuel cell system ( $P_{Net}$ ) while compressor voltage ( $V_{Cp}$ ) as a second input is used to control compressor speed which regulates the oxidant flow rate and supplied reactant into the stack. Net power is the main controlled variable while the oxygen excess ratio ( $\lambda_{O_2}$ ) is selected as an auxiliary controlled variable which has

a considerable effect on power dynamics and fuel cell life. In the following sections, the details of the controller configurations are presented.

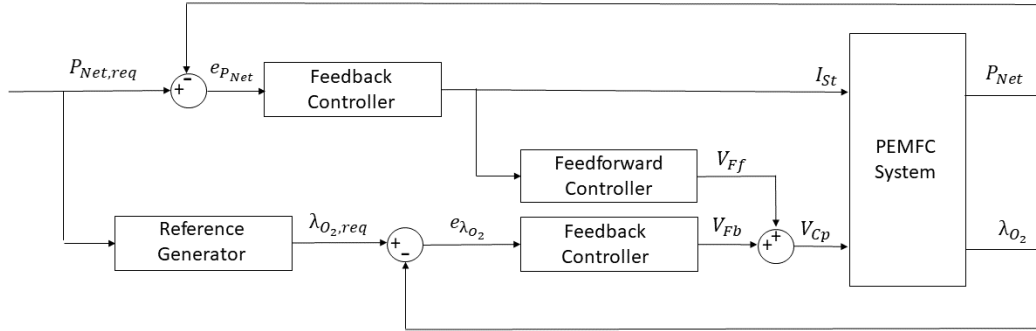


**Figure 3.7 :** Proposed control system architecture for the PEM fuel cell system.

### 3.2.1 Control system requirements

Model developed specifically for control studies have certain characteristics. Important characteristics such as dynamic (transient) effects are included. Some other effects, such as spatial variation of parameters, are lumped and included as ordinary differential or static equation forms. Furthermore, only dynamic effects that are related to automobile operations are integrated into the models. The relevant time constant for an automotive propulsion-sized PEM fuel cell system are summarized in table 3.1.

**Table 3.1 :** Time constants of various dynamics [2].

Type of Dynamics	Time Constant (s)
Electrochemistry	$10^{-19}$
Hydrogen & air manifolds	$10^{-1}$
Membrane water content	Unclear
Flow control/supercharging devices	$10^0$
Vehicle inertia dynamics	$10^1$
Cell and stack temperature	$10^2$

Since the fuel cell system isolated from automotive powertrain and operation at constant temperature is simulated, the time constants associated with vehicle inertia and temperature variations can be disregarded. Thus, the system time constant order is predominantly identified by dynamics of flow control. The system outputs, namely net power generation and oxygen excess ratio, are crucial considerations in power

management. These variables exhibit a dynamic interrelationship wherein alterations in one parameter can significantly impact the other. However, emphasizing the regulation of power output is paramount due to its role as the primary controlled variable. Consequently, the control of oxygen excess ratio takes precedence over power output regulation to ensure optimal system performance and stability. Hence, the control system is engineered to achieve an oxygen excess ratio settling time of less than 1 second with an acceptable overshoot of less than 10%. Simultaneously, the power output is targeted to reach its steady-state value within 2 seconds, devoid of any overshoot, to mitigate the risk of excessive power generation. These precise specifications are established to uphold operational stability and success criteria of the performance of the control system.

### 3.2.2 Power controller configuration

The fuel cell system generates power under the request of vehicle control unit. The actual generated power from fuel cell system is fed back to the controller and error term for net power ( $e_{P_{Net}}$ ) is created. As power feedback controller, classic type PI controller is selected (3.3). The Proportional ( $K_P$ ) and Integral ( $K_I$ ) coefficients of PI controller is tuned according to the power settling time requirement in the previous section and tuning result for the controller parameters presented in the table 3.2.

$$G_{P_{Net}}(s) = \frac{K_I}{s} + K_P \quad (3.3)$$

**Table 3.2 :** PI controller tuning result for power controller.

Coefficient	Value
$K_P$	0.3
$K_I$	10

### 3.2.3 Oxygen excess ratio controller configuration

Oxygen excess ratio control is comprised of 3 steps. Firstly, reference value is obtained by data-driven map which is experimentally obtained. Secondly, for a fast and disturbance free reaction, static feedforward controller is used to create compressor

voltage based on stack current. Finally, feedback controller is added to increase the accuracy. In the following sections, the configurations are detailed.

### 3.2.3.1 Reference generator for oxygen excess ratio

Ensuring optimized oxygen excess ratios is crucial for efficient power generation. Kendir’s study [6] establishes a correlation between maximum net power output and oxygen excess ratio, illustrated in Fig. 3.8.

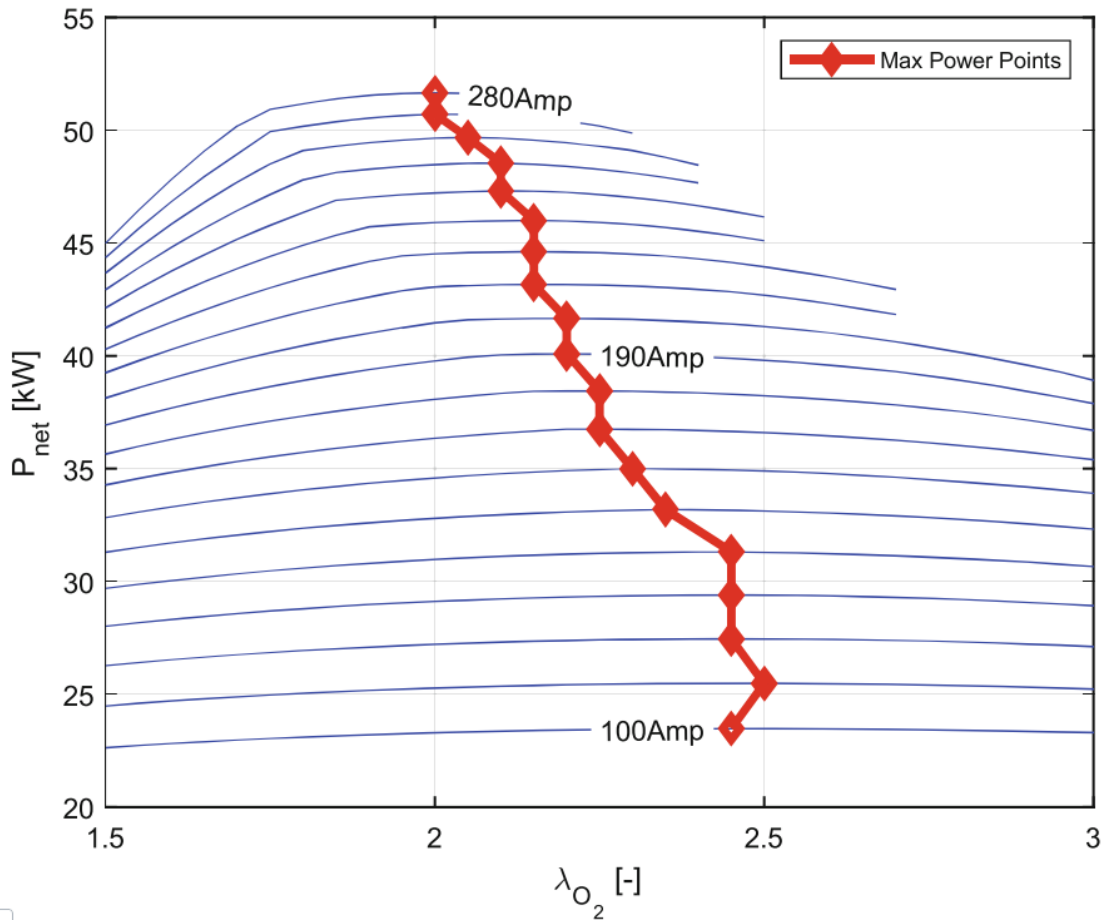


**Figure 3.8 :** The maximal power points corresponding to different OER points [6].

Additionally, a data-driven reference generator is devised in the same study to determine the ideal oxygen excess ratio corresponding to specific stack currents. This is achieved by conducting experiments with constant stack currents while measuring both output power and oxygen excess ratio. However, due to the dynamic nature of power change requests, a closed-loop control system brings additional transients to the

stack current. Consequently, instead of directly correlating oxygen excess ratio with stack current, the reference generator calculates reference oxygen excess ratio based on power. The relation between power request to oxygen excess ratio is implemented with a look up table, as in Fig. 3.9.

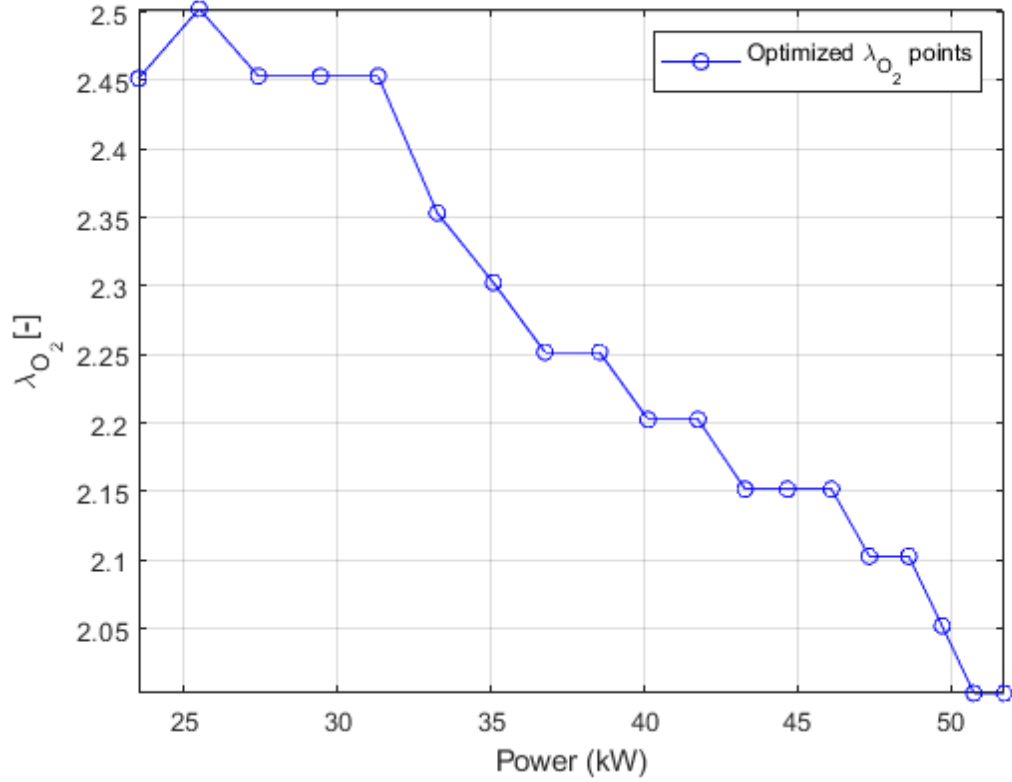


**Figure 3.9 :** Optimal OER points corresponding to the power request points.

### 3.2.3.2 Feedforward controller

It is beneficial to add a feedforward controller to react disturbance. The current acts as a disturbance to  $\lambda_{O_2}$ . A static function correlated with the the control input,  $V_{Ff}$ , and the disturbance,  $I_{St}$ , could be used in the feedforward path as in the [3]. This static feedforward is implemented with polynomial function (3.4). Thereafter, the feedforward term of compressor voltage ( $V_{Ff}$ ) is added into feedback term ( $V_{Fb}$ ) to obtain the main control input of compressor voltage ( $V_{Cp}$ ).

$$V_{Ff} = 0.6725.I_{St} + 35.5541 \quad (3.4)$$

### 3.2.3.3 Feedback controller

Besides the feedforward controller, feedback controller is added to increase the accuracy oxygen excess ratio during steady state condition. Several configurations and tuning results are presented in the following section.



## 4. SIMULATIONS AND RESULTS

In this chapter, feedback controller configurations are compared similar to [23]. First, the initial configuration, classical PI controller configuration and tuning results, are presented. Afterward, an advanced controller method, fuzzy logic-based PID controllers, is presented to improve the transient response of OER. For the fuzzy logic controllers, scaling coefficients for type-1, and the footprint of uncertainty coefficients for type-2 is heuristically tuned. Finally, several configurations results are compared in terms of OER, power transients and system overall efficiency.

As classic PID controllers dominate the control operations in the industry, it is selected as the initial option in the use of feedback controllers. PI configuration is selected because derivative effects of reference signal deteriorates the closed loop performance due to non-minimum phase dynamics of fuel cell system [3]. Fortunately, a feedforward controller is used besides the feedback controller to present the derivative effect. The derivative coefficient ( $K_D$ ) value is selected as 0, and the PID configuration is reduced to PI.

### 4.1 Classic PI Controller

Due to nonlinear time variant system characteristics, model-based and analytical tuning methods are omitted and for PI controller tuning, Proportional ( $K_P$ ) and Integral ( $K_I$ ) configurations are determined heuristically. As an initial value, the  $K_I$  is selected 300 and  $K_P$  values between 10 to 100 is tested. The reference OER value is stepped from 2.20 to 2.29 (OER reference generator transformation from 35 to 40 kW) and actual OER responses are compared as shown in the Fig. 4.1. The settling time of the  $K_P$  configurations resulted with similar, however the transient effects are different. For the higher  $K_P$  values, jumping behaviour is intensified after reference change, even some of entering 2% band for a moment. For the lower  $K_P$  values, these behaviours are

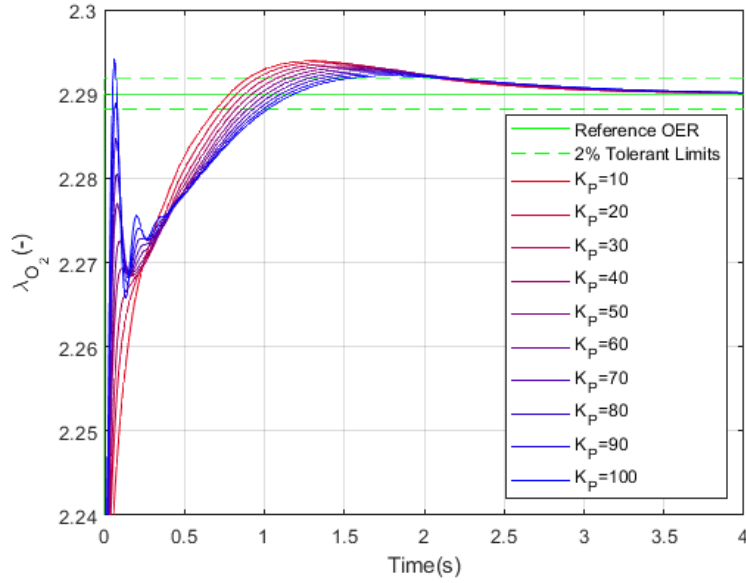


**Figure 4.1 :**  $K_P$  tuning test for classic PI controller,  $K_I = 300$ .

less observed, however, overshoot is higher compared to the higher  $K_P$  values. Since the earlier oscillations and higher overshoot amplitude do not preferred much,  $K_P$  value is chosen from a mid range value, such as 30 for PI configuration.

After the determination of  $K_P$ , the  $K_I$  value is tuned. The range of tested  $K_I$  values are between 250 to 800 as shown in the Fig. 4.2. In the lower values of  $K_I$ , the settling time and overshoot are higher. As the  $K_I$  value increases, both of them get better; however, jumping is started to be observed. Therefore,  $K_I$  value is selected to a closer value of higher ones, as 500. Finally, the  $\lambda_{O_2}$  feedback controller (4.1) coefficients are tuned as presented in the following table 4.1.

$$G_{\lambda_{O_2}}(s) = \frac{K_I}{s} + K_P \quad (4.1)$$

**Table 4.1 :** PI controller tuning result for OER controller.

Coefficient	Value
$K_P$	30
$K_I$	500

As can be seen in the Fig. 4.3, despite the OER enter 2% tolerance band, there is a small overshoot observed, and enters the band again in 1.6 seconds again. Therefore, the settling time of the OER results with 1.6 seconds with maximal 3% overshoot. As

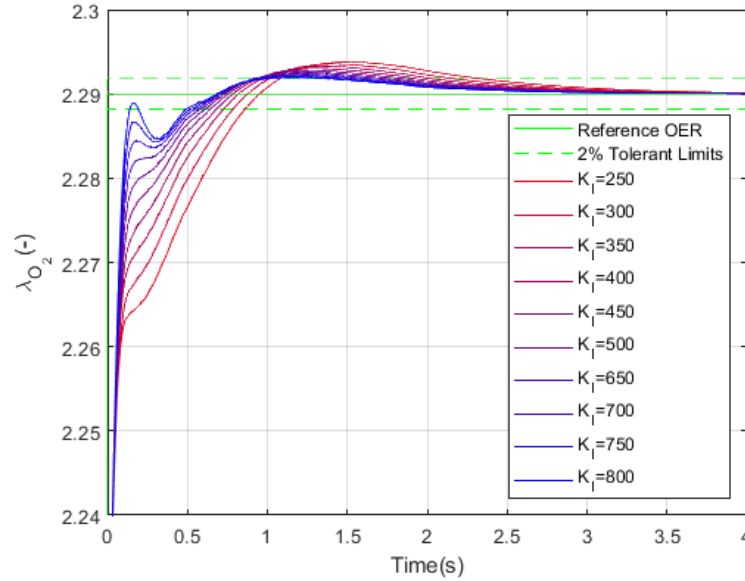


**Figure 4.2 :**  $K_I$  tuning test for classic PI controller,  $K_P = 30$ .

proposed in the section 3.2.1, the settling time purpose is set to 1 seconds. Therefore, there is an effort to replace classical PI controller with an advanced controller. In the next section, fuzzy logic based PID controller structure is presented.

#### 4.2 Fuzzy Logic Based PID Controller

In addition to classical structure, PID controllers have recently gained prominence with advanced methods. Fuzzy logic-based PID controllers have become suitable for nonlinear control due to their fuzzy logic structure and, therefore, have become widely used in industry. In recent years, numerous studies have emerged in this field, and ready-made software solutions have been developed. One of these [24] has been used as an alternative to the classical PI controller in this study. This study offers an open-source toolbox to design both type-1 and interval type-2 fuzzy logic-based controllers. The fuzzy PID controller architecture is presented in Fig. 4.4.

Fuzzy logic PID controller consists of fuzzy logic controller, scaling coefficients of  $C_e$  for normalizing error,  $C_d$  for normalizing derivative of error,  $C_0$  for integral gain, and  $C_l$  for proportional gain. The fuzzy logic controller output ( $U$ ) is calculated based scaled error( $E$ ) and derivative of error( $\Delta E$  or  $deE$ ) according to the relationship with membership function. Using gains of  $C_0$ ,  $C_l$ , the  $U$  is scaled with integral and

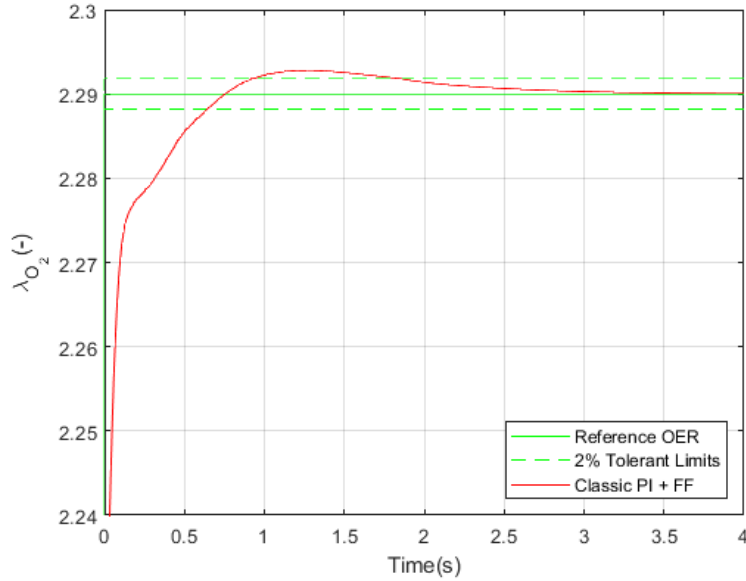


**Figure 4.3 :** OER response of the selected configuration of classic PI controller,  $K_P=30$ ,  $K_I=500$ .

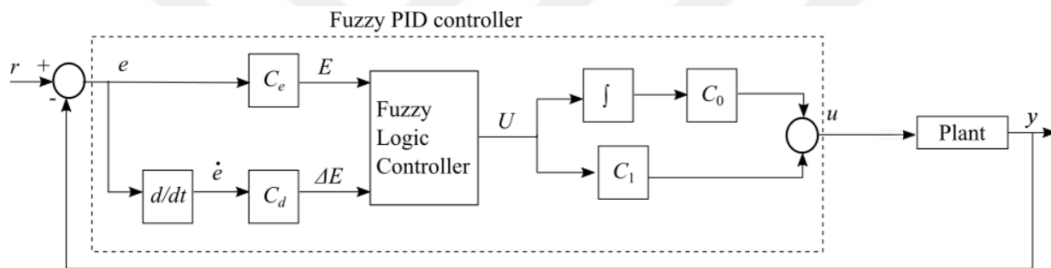
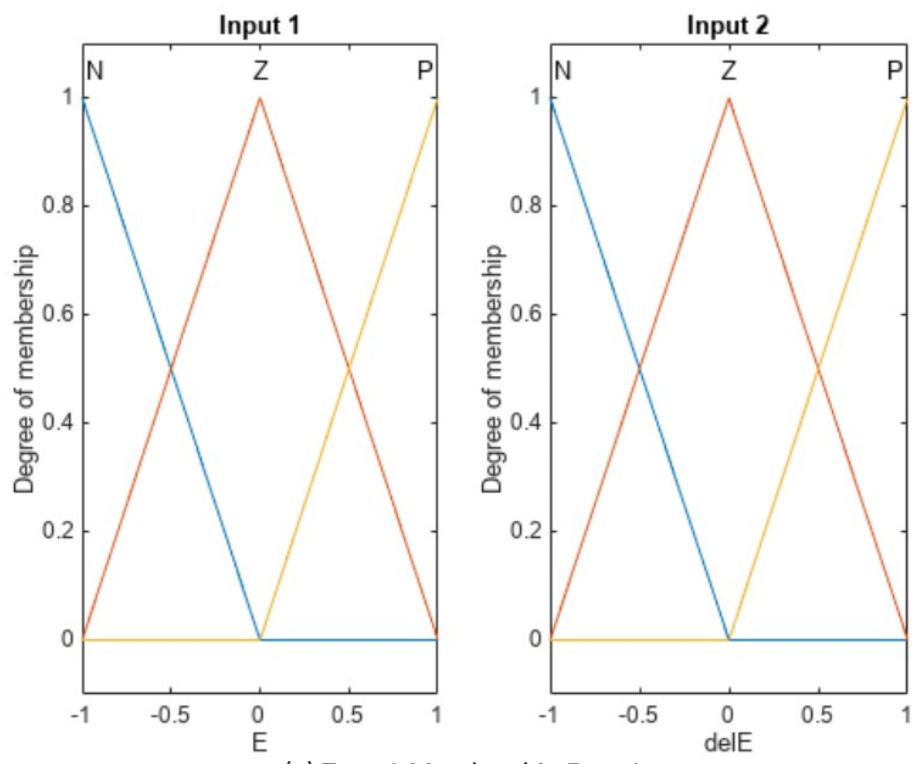


**Figure 4.4 :** Fuzzy logic based PID controller architecture [7].

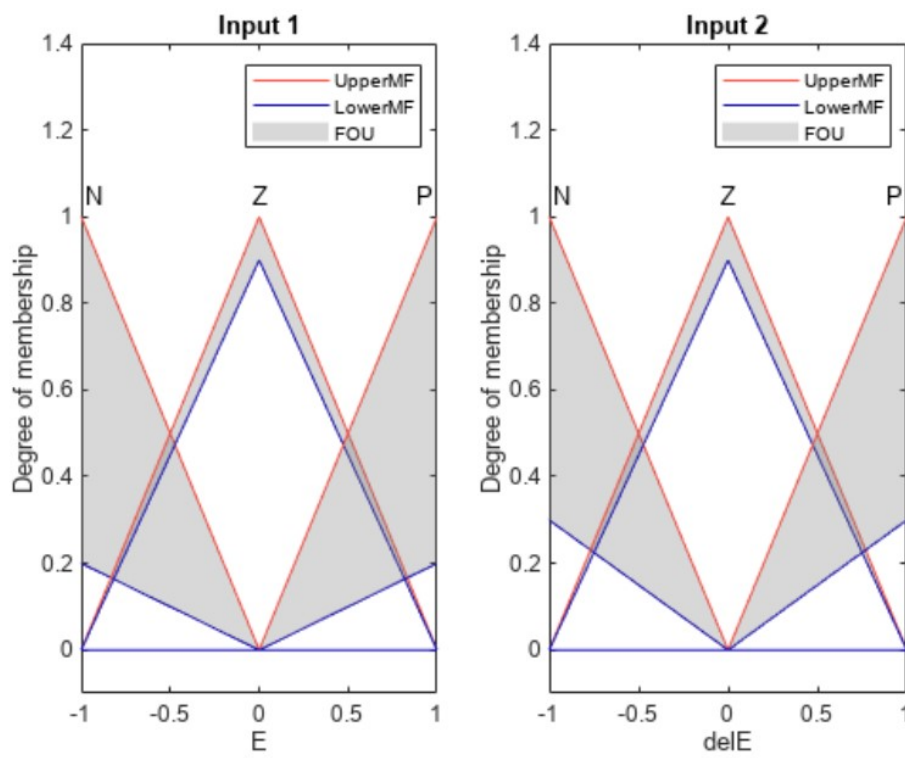
proportional coefficients and final control output value ( $u$ ) is obtained. The fuzzy set of membership functions determines the type of fuzzy logic controller. As can be seen from Fig. 4.5(a), strictly defined membership degrees are called type-1, while uncertainty included and interval value defined membership degrees as in Fig. 4.5(b) are called interval type-2 fuzzy logic controllers. Tuning of scaling coefficients and footprint of uncertainty coefficients brings an additional degree of freedom. In the following section, the test results for the tuning study of these coefficients are presented.

#### 4.2.1 Fuzzy logic controller

The fuzzy logic controller consists of identical 3 membership functions(MFs) for the inputs  $E$  and  $dE$ . The input membership functions are defined in triangular type as



(a) Type-1 Membership Function



(b) Type-2 Membership Function

**Figure 4.5 :** Type-1 and Type-2 input membership function definitions [7].

seen in Fig. 4.5. N, Z, and P correspond to Negative, Zero, and Positive in table 4.2. There are 5 constant membership functions defined for the output. NB, NM, Z, PM, and PB correspond to Negative-Big, Negative-Medium, Zero, Positive-Medium, and Positive-Big in table 4.3. The rules and property settings of the fuzzy logic controller are presented in table 4.4 and 4.5. For the type-2 controller settings, lower degree values are additionally defined in section 4.2.3. The Karnik Mendel Method is selected as the type-reduction method for the type-2 controller.

**Table 4.2 :** Fuzzy logic controller input membership function definition.

Name	Type	Parameters
<i>N</i>	Triangular	[-2 -1 0]
<i>Z</i>	Triangular	[-1 0 1]
<i>P</i>	Triangular	[0 1 2]

**Table 4.3 :** Fuzzy logic controller output membership function definition.

Name	Type	Parameters
<i>NB</i>	Constant	-1
<i>NM</i>	Constant	-0.5
<i>Z</i>	Constant	0
<i>PM</i>	Constant	0.5
<i>PB</i>	Constant	1

**Table 4.4 :** Fuzzy logic controller rule definition.

#	Rule
1	If E is N and delE is N then U is NB
2	If E is Z and delE is N then U is NM
3	If E is P and delE is N then U is Z
4	If E is N and delE is Z then U is NM
5	If E is Z and delE is Z then U is Z
6	If E is P and delE is Z then U is PM
7	If E is N and delE is P then U is Z
8	If E is Z and delE is P then U is PM
9	If E is P and delE is P then U is PB

#### 4.2.2 Setting of scaling coefficients

In the first study of fuzzy PID controller tuning, the effect of gain coefficients of  $C_0$  and  $C_l$  is investigated. The input membership functions defined in Fig. 4.5(a) are used.  $C_e$  and  $C_d$  are set to 1.  $C_0$  is set to values between 450 and 1000, while  $C_l$  is 200 as an

**Table 4.5 :** Fuzzy logic controller fuzzy inference setting.

Property	Definition
Type	Sugeno Type-1
And method	Product
Or method	Probabilistic
Implication method	Product
Aggregation method	Sum of the rule output sets
Defuzzification method	Weighted average of all rule outputs

initial value. For the lower values of  $C_0$ , the settling time is high, while on the other hand overshoot is comparatively high for the higher values of  $C_0$  as can be seen from the Fig. 4.6. As a result, 700 gives the optimal result in terms of settling time and overshoot for the  $C_0$ .

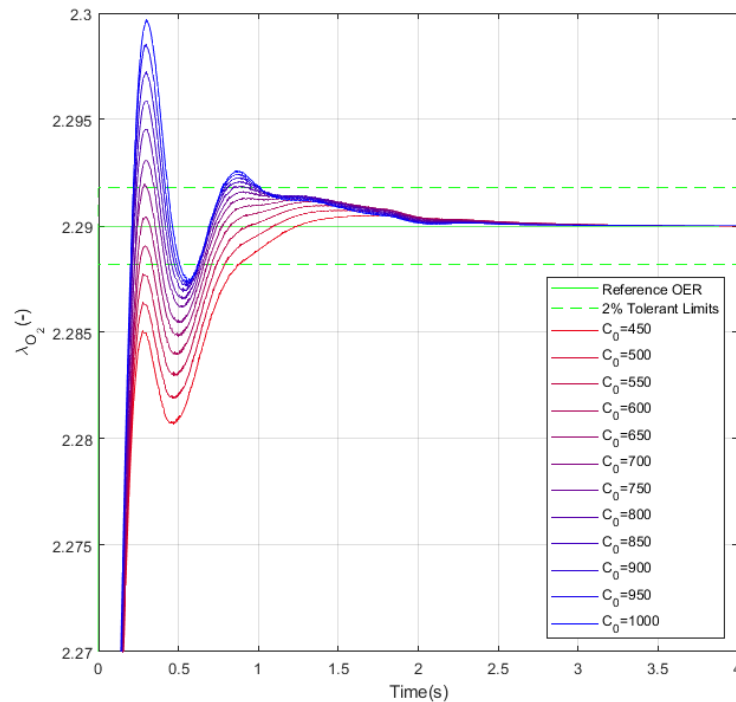


**Figure 4.6 :**  $C_0$  tuning test for type-1 controller,  $C_l = 200$ .

After tuning of integral coefficient, proportional gain is tuned.  $C_l$  is set to values between 170 and 270. The effect of proportional gain on the settling time is inconsiderable, however undershoot tendency is increased when the  $C_l$  gets higher values. Undershoot up to lower 2% tolerance limit is allowed, and 240 is considered

as giving optimal result for the  $C_I$  according to the Fig. 4.7. The tuning results are presented in Fig. 4.8 and table 4.6.

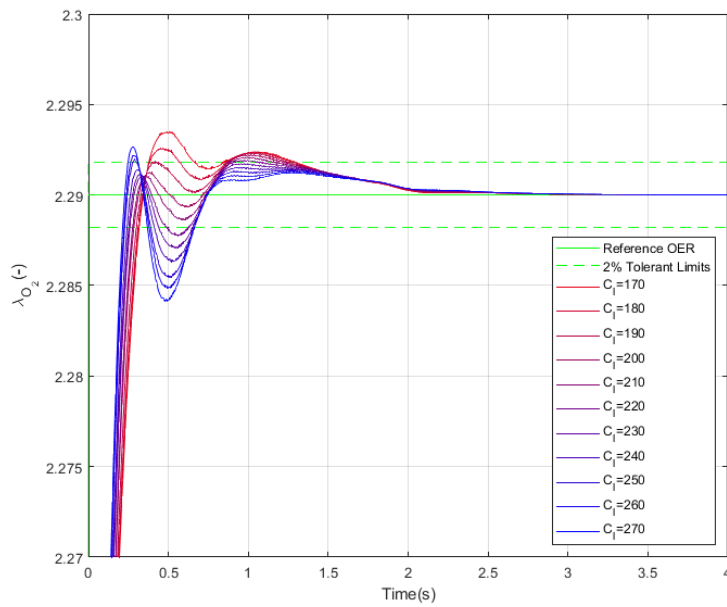


**Figure 4.7 :**  $C_I$  tuning test for type-1 controller,  $C_0 = 700$ .

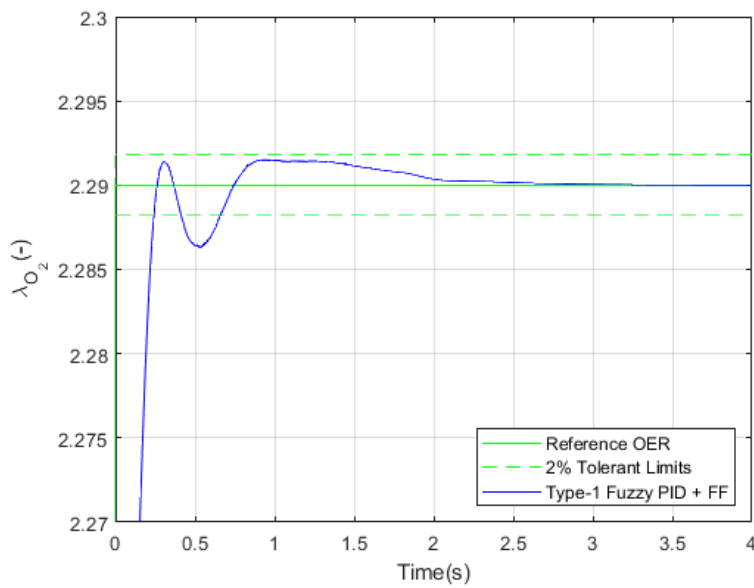


**Figure 4.8 :** OER response of the selected configuration of fuzzy type-1 PID controller,  $C_0 = 700$ ,  $C_I = 240$ .

**Table 4.6 :** Fuzzy PID controller tuning result for gain coefficients.

Coefficient	Value
$C_0$	700
$C_I$	240

### 4.2.3 Setting of footprint of uncertainty coefficients

In the second study of fuzzy PID controller tuning, the effect of footprint of uncertainty coefficients is investigated. As can be seen from the Fig. 4.5(b), membership function area(gray) is limited within upper and lower degree values. Adding a lower degree value is the fundamental distinction of type-2 from type-1 fuzzy logic controller, and it adds additional degree of freedom for the controller design. This study analyses the effect of changing lower degree values on transient response of the OER. In total, there are 6 lower degree values for N,Z,P of input 1 and N,Z,P of input 2; however, it is reduced to 4 via combining N and P lower degree values both for input 1(E) and 2(delE). The values are called as  $z_1, z_2, z_3$  and  $z_4$  corresponding to the lower degree values of (N,P), Z for input 1 and (N,P), Z for input 2 respectively.

In Fig. 4.9,  $z_1$  is set to values between 1 and 0.2. As the  $z_1$  value gets lower values, first oscillation amplitude reduces, but this also results with higher settling time.

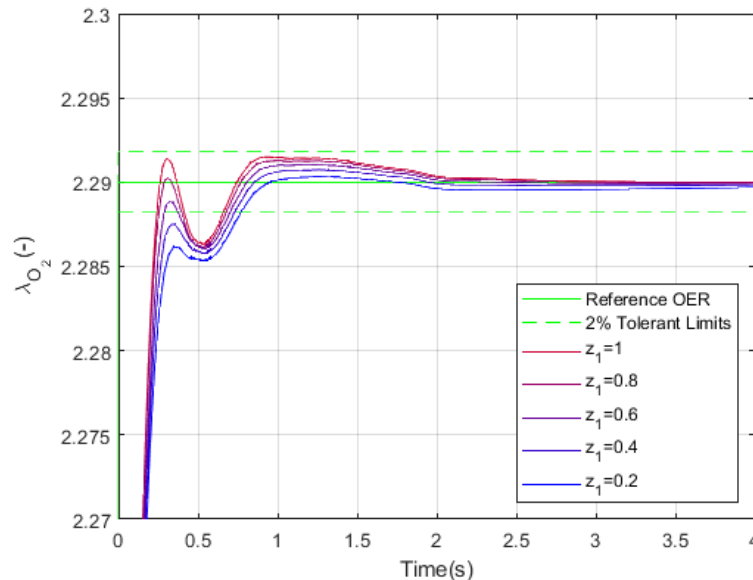


**Figure 4.9 :**  $z_1$  tuning test for type-2 controller.

In Fig. 4.10,  $z_2$  is set to values between 1 and 0.4. As the  $z_2$  gets lower values, the response is more oscillating and overshoot amplitudes increase.

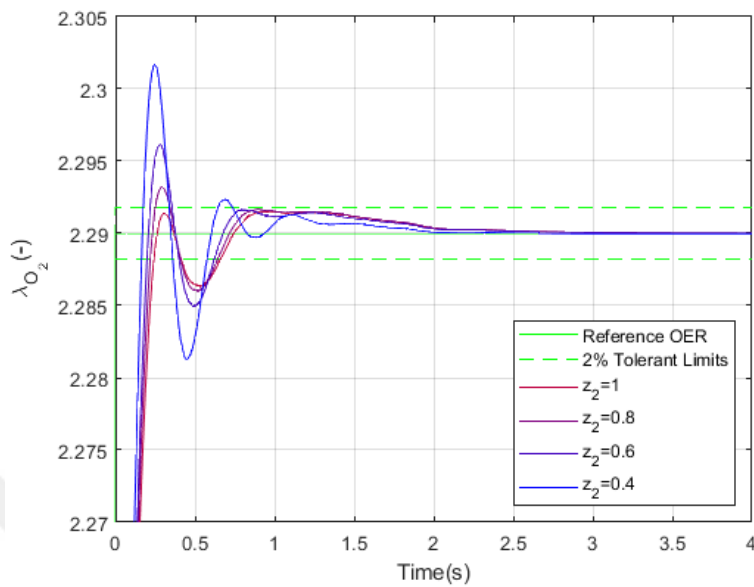


**Figure 4.10 :**  $z_2$  tuning test for type-2 controller.

In Fig. 4.11,  $z_3$  is set to values between 1 and 0.4. As the  $z_3$  gets lower values, the undershoot tendency is reduced, but overshoot with higher amplitudes from 2% tolerance band is observed in the second oscillation.

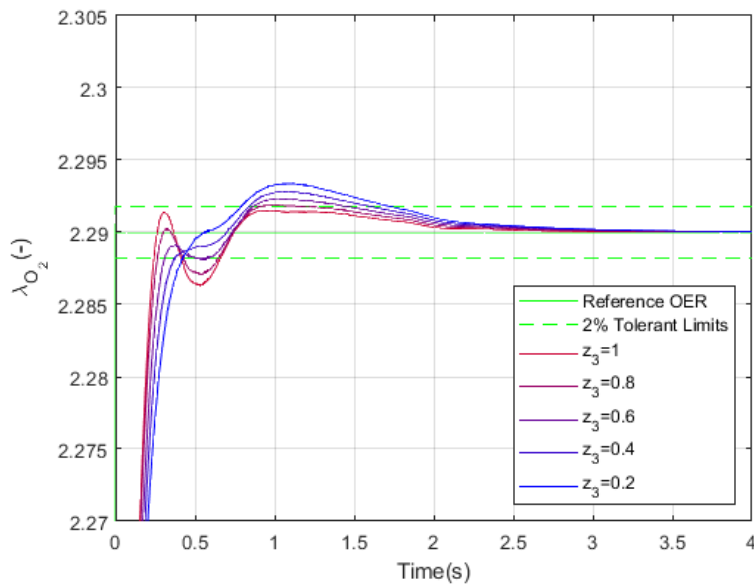


**Figure 4.11 :**  $z_3$  tuning test for type-2 controller.

In Fig. 4.12,  $z_4$  is set to values between 1 and 0.4. As the  $z_4$  gets lower values, the response is more oscillating, similar to  $z_2$  result. Setting  $z$  values in lower values do not give better results compared to  $z$  is 1, which corresponds type-1 fuzzy controller setting. Therefore, adding additional degree via using type-2 fuzzy controller lower membership degree values has resulted with no improvement on the transient response. Since type-1 fuzzy controller results with the best OER transient, it is replaces classic PI controller for feedback controller, and selected as the final configuration for the feedback controller. In the next section, this configuration is analysed in detail with comparing different configurations.

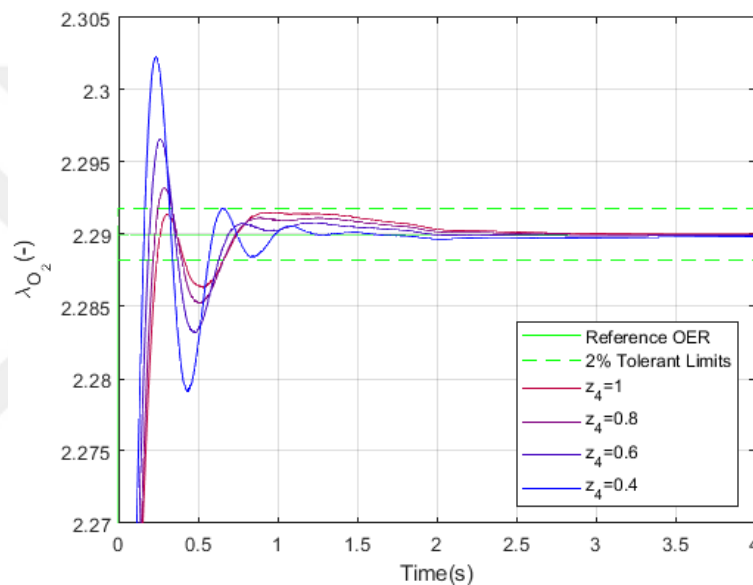


**Figure 4.12 :**  $z_4$  tuning test for type-2 controller.

### 4.3 Comparison of All Controller Configurations

In the previous sections, the control system architecture of the PEM fuel cell system is presented, and the type-1 PID controller is chosen as the feedback controller. For OER control, this control strategy is tested against 3 different configurations. Fuzzy type-1 PID feedback plus feedforward controller is compared against classic PI feedback plus feedforward controller, single feedforward controller, and single classical PI feedback controller performances. In test scenario, net power request is rising from 35 kW to 40 kW, while OER request is changing from 2.2 to 2.9 after reference generator

calculation. The control inputs corresponding to different configurations are presented in Fig. 4.13 and Fig. 4.14.

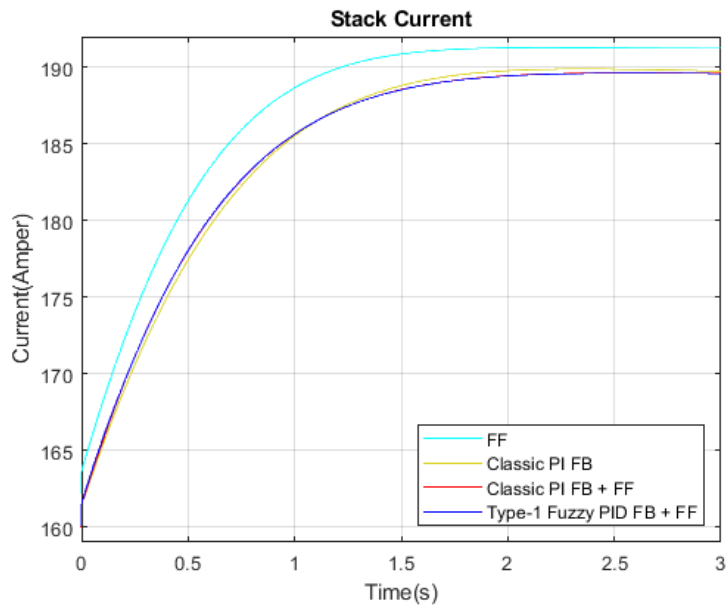


**Figure 4.13 :** Stack current input for different configurations.

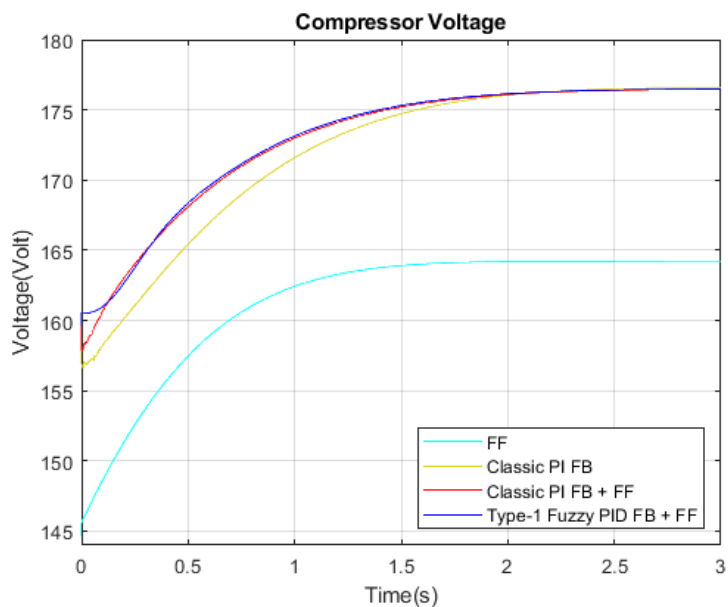


**Figure 4.14 :** Compressor voltage input for different configurations.

In Fig. 4.15, the OER responses of all controller configurations are presented. It can be seen that all controller configurations except feedforward goes to the reference value of OER. The feedforward controller has been previously designed to keep the OER constant, which is 2, in different power scenarios, but even there, steady-state error is

observed due to the lack of feedback. Classic PI controller OER response enters into the 2% tolerance within 2.3 seconds after reference changing, but with a significant overshoot, around 30%. Using a feedforward controller seems convenient to reduce both settling time and overshoot amplitude, as can be seen for feedback(FB) with feedforward(FF) controller configurations in Fig. 4.15.

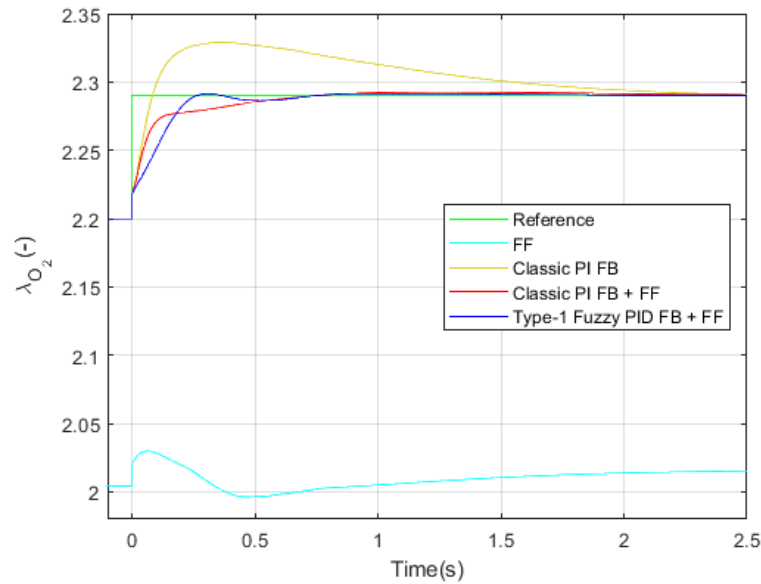


**Figure 4.15 :** Comparison of OER step responses for several controller configurations.

Consequently, the deviation from reference measured by integral absolute error(IAE) is considerably reduced with feedback plus feedforward configuration, as seen from table 4.7.

**Table 4.7 :** OER performance statistics for all controller configurations.

Configuration	IAE(-)	Settling Time(s)	Overshoot(%)
Feedforward	1.3851	-	-
Classic PI	0.0463	2.29	33
Classic PI + Feedforward	0.0135	1.85	3.1
Fuzzy PID + Feedforward	0.0123	0.67	1.5

In Fig. 4.16, the feedback with feedforward controllers OER responses are examined in more detail. From the requirements perspective, type-1 fuzzy PID results with better transients for OER. Compared to 1.8 seconds of classical PI controller, fuzzy controller results with 0.7 seconds settling time with less overshoot. For classic PI

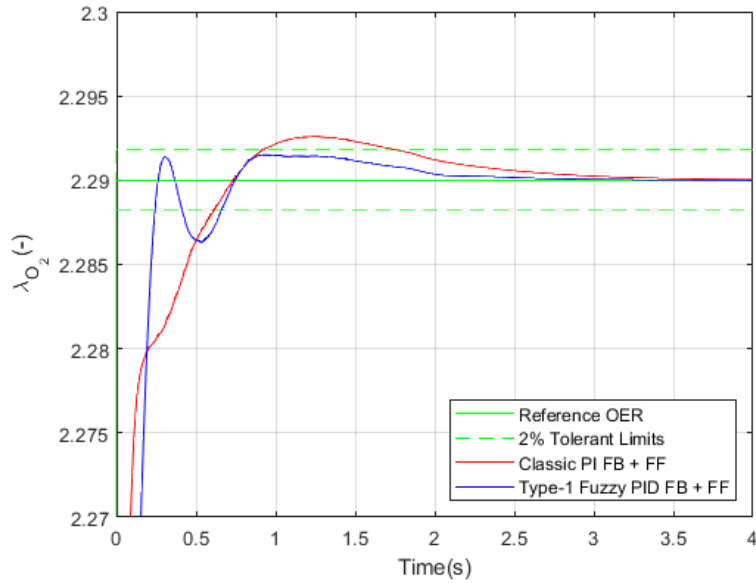


**Figure 4.16 :** Comparison of OER responses for classic and fuzzy type-1 feedback controllers.

controller, overshoot is observed over the 2% tolerant limit, and settling time is almost 1 second later than the fuzzy controller configuration. OER performance results are summarized in table 4.7. Trade-off between OER and net power dynamics, brings slower power response for fuzzy PID controller compared to classic PI controller, as seen from Fig. 4.17.

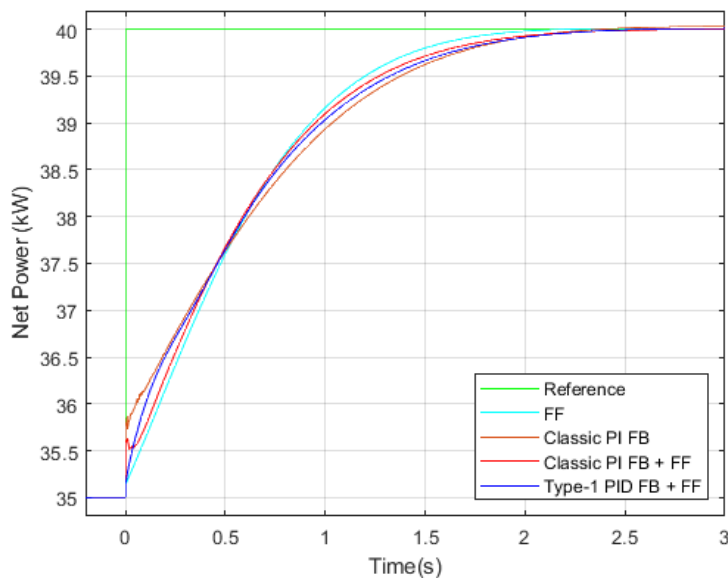


**Figure 4.17 :** Comparison of power step responses for several controller configurations.

However, the difference in settling time 0.1 second, which is negligible. The 2 second settling time requirement for power is satisfied for all controller configurations with minor differences. After reference change, all power responses settled in the 2% tolerant limits within 2 seconds, according to Fig. 4.17. Power performance results are summarized in table 4.8.

**Table 4.8 :** Power performance statistics for all controller configurations.

Configuration	IAE(-)	Settling Time(s)	Overshoot(%)
Feedforward	2.9088	1.68	0.17
Classic PI	3.0095	1.95	0.60
Classic PI + Feedforward	2.9709	1.85	0.01
Fuzzy PID + Feedforward	2.9673	1.95	0.22

Finally, the efficiency plots of all the configurations are presented within Fig. 4.18. As expected, feedback included configurations are superior than the excluded ones, which is singular feedforward, in terms of efficiency due to usage of optimal reference OER. The overall system efficiency is between 44-50% range, and 45.8% in 40 kW steady state conditions for the feedback controller included configurations.

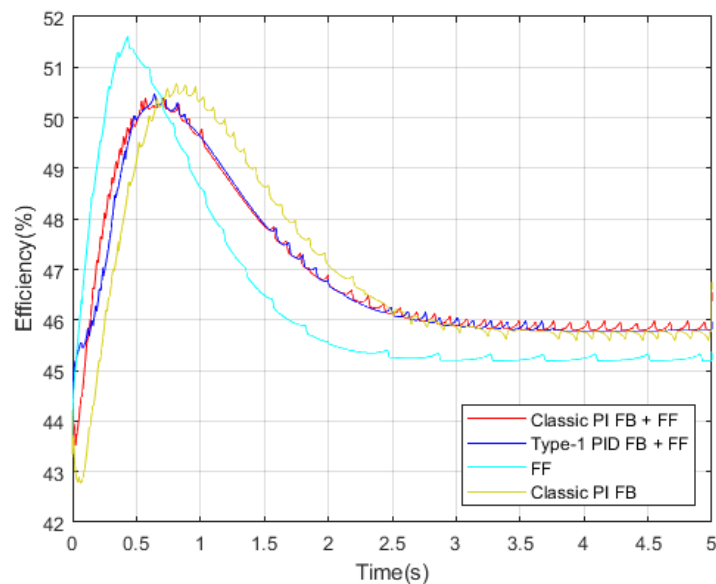


**Figure 4.18 :** System efficiency comparison for several controller configurations.

The efficiency statistics are summarized in table 4.9. Despite table 4.8 presents top power performance is provided with isolated feedforward controller, efficiency is ended around 45.2% at steady state, which is low compared to the feedback included

ones. Improvement in efficiency with the reference generator and feedback controller is almost 0.6%, with a slight performance deterioration for settling time, about 0.2 seconds. According to the results, type-1 fuzzy based PID controller with feedforward controller satisfies all the requirements, and selected as the proposed control method for this study.

**Table 4.9 :** Efficiency performance statistics for all controller configurations.

Configuration	Mean (%)	Max(%)	Steady State(%)
Feedforward	46.45	51.61	45.19
Classic PI	46.49	50.66	45.78
Classic PI + Feedforward	47.35	50.39	45.79
Fuzzy PID + Feedforward	46.86	50.46	45.79



## 5. CONCLUSIONS

This study proposes a power control strategy for fuel cell systems to maximize system efficiency with improved OER dynamics. The strategy includes PI feedback controller for net power; and feedforward controller supported fuzzy type-1 PID feedback controller and data-driven based reference generator for OER. The control strategy is promising to prevent instant oxygen starvation via avoiding sudden drops in OER levels, and offer longer lifespan for fuel cell stack. The control strategy is tested on fuel cell system model package from Michigan University. The model is composed of stack, compressor and the other auxiliary component models to simulate power generation from fuel cell system with reactant flows. The model is utilized as 2-input-2-output model, OER and net power as outputs and stack current and compressor voltage as inputs. The control system aims to maximize system efficiency by operating at optimal OER that maximizes net power generation. Independent feedback controllers are implemented for OER and net power. To provide optimal OER, look-up table based reference OER generator is implemented. Reference OER generator is derived via sampling of the OER values resulting peak power generation for various load currents. A static feedforward controller accompanying OER feedback controller is implemented to compensate the disturbance effect of stack current into OER performance, and to obtain faster response. Thereby during tests, sudden drops in OER levels are not observed, and settling time is considerably improved with contribution of feedforward controller. Feedback controllers are designed according to the criteria considering system dynamics limits. Settling time of 1 second with overshoot allowance for OER control, and 2 seconds without overshoot is determined as control system requirements. Tuned classic PI controller gives sufficient results for power loop. For OER control, classic PI controller with feedforward implementation results in 1.6 second settling time. To improve transients, classical PID controller couldn't be used due to its derivative term causing instability for fuel cell system,

because of non-minimum phase characteristics. As a solution, instead of a linear controller, an advanced nonlinear controller is used to convert PI into PID. Fuzzy type PID controller is utilized due to its suitability for nonlinear dynamics, and advantages of additional degree of freedom. Fuzzy type-1 controller with scaling coefficients and fuzzy type-2 controller with footprint of uncertainty coefficients are heuristically tuned. Despite of additional degrees of type-2, type-1 PID controller brings better results. Therefore, Type-1 Fuzzy PID controller is utilized as feedback controller, besides feedforward controller. The implementation ends with 0.7 and 1.95 second settling times without overshoot for OER and net power, which satisfies transient dynamic criteria for both of them. An efficiency formula is derived and implemented within model to measure the the effectiveness of the proposed strategy. The system running at 35-40 kW indicates 45 to 50% efficiency according to this formula. Ensuring optimal OER conditions with reference generator and feedback controller implementation results in 0.6% efficiency increase compared to an operation at a fixed OER without feedback.

The study is open for future improvements. First of all, the optimality of the controller tuning can be guaranteed by other optimisation methods. Heuristic tuning approach is preferred for classical and fuzzy PID controllers. The selected range of coefficients does not guarantee global optimality, but local. Utilizing an optimisation method either deterministic or stochastic approach can bring better results. Due to complexity of fuel cell model with nonlinear dynamics, model based approaches are not recommended, but data-driven optimization methods based on experiments will be more convenient, and applicable solution for industrial applications. Secondly, the proposed control strategy is tested on a narrow operational condition, around 35 - 40 kW. Nonlinear dynamics dependent on operational conditions can cause differentiation of system characteristics from tested conditions in this study. To increase the robustness and guarantee the performance, tuning mechanisms can be added, such as online gain

scheduling. Finally, electrochemical impedance spectroscopy can be utilized to show the effectiveness of the proposed control strategy as a degradation mitigation strategy.





## REFERENCES

- [1] **U.S. Department of Energy** (n.d.). *Types of Fuel Cells*, <https://www.energy.gov/eere/fuelcells/types-fuel-cells>, accessed April 15, 2024.
- [2] **Guzzella, L.** (1999). Control oriented modelling of fuel-cell based vehicles, *Presentation in NSF Workshop on the Integration of Modeling and Control for Automotive systems*, The University of Michigan, US, p.n.d.
- [3] **Pukrushpan, J.T.** (2003). *Modeling and control of fuel cell systems and fuel processors*, University of Michigan.
- [4] **Dervisoglu, R.** (2020). *Scheme of a proton-conducting fuel cell*, [http://en.wikipedia.org/wiki/File:Solid\\_oxide\\_fuel\\_cell.svg](http://en.wikipedia.org/wiki/File:Solid_oxide_fuel_cell.svg), accessed May 2, 2024.
- [5] **Adams, J.A., Yang, W.c., Oglesby, K.A. and Osborne, K.D.** (2000). The development of Ford's P2000 fuel cell vehicle, *SAE Transactions*, 1634–1645.
- [6] **Kendir, F. and Kumbasar, T.** (2023). Design of 2 DOF fuzzy control system for fuel cell systems, *International Conference on Intelligent and Fuzzy Systems*, Springer Nature Switzerland, Cham, pp.584–591.
- [7] **Mendel, J.M.** (2017). *Uncertain rule-based fuzzy systems. Introduction and new directions*, volume 684, Springer International Publishing.
- [8] **Taniguchi, A., Akita, T., Yasuda, K. and Miyazaki, Y.** (2008). Analysis of degradation in PEMFC caused by cell reversal during air starvation, *International Journal of Hydrogen Energy*, 33(9), 2323–2329.
- [9] **Gerard, M., Poirot-Crouvezier, J.P., Hissel, D. and Pera, M.C.** (2010). Oxygen starvation analysis during air feeding faults in PEMFC, *International Journal of Hydrogen Energy*, 35(22), 12295–12307.
- [10] **Wu, J., Yuan, X.Z., Martin, J.J., Wang, H., Zhang, J., Shen, J., Wu, S. and Merida, W.** (2008). A review of PEM fuel cell durability: Degradation mechanisms and mitigation strategies, *Journal of Power Sources*, 184(1), 104–119.
- [11] **Pukrushpan, J.T., Stefanopoulou, A.G. and Peng, H.** (2002). *University of Michigan Fuel Cell Stack Simulation package*, University of Michigan, <https://hdl.handle.net/2027.42/90423>, accessed: March 29, 2024.

- [12] **Yin, P., Chen, J. and He, H.** (2018). Control of Oxygen Excess Ratio for a PEMFC Air Supply System by Intelligent PID Methods, *Sustainability* 2023, 15(11), 8500.
- [13] **Li, M., Lu, J., Hu, Y. and Gao, J.** (2018). Oxygen excess ratio controller design of PEM fuel cell, *IFAC-PapersOnLine*, 51(31), 493–498.
- [14] **Ma, L., Zhao, H., Qu, Y., Zhao, S., Yu, Y. and Wei, W.** (2023). Reduced-order active disturbance rejection control method for PEMFC air intake system based on the estimation of oxygen excess ratio, *IET Renewable Power Generation*, 17(4), 951–963.
- [15] **Grove, W.R.** (1839). XLII. On a small voltaic battery of great energy; some observations on voltaic combinations and forms of arrangement; and on the inactivity of a copper positive electrode in nitro-sulphuric acid, *The London, Edinburgh, and Dublin Philosophical Magazine and Journal of Science*, 15(96), 287–293.
- [16] **Bacon, F.T.** (1969). Fuel cells, past, present and future, *Electrochimica Acta*, 14(7), 569–585.
- [17] **Dodds, P.E., Staffell, I., Hawkes, A.D., Li, F., Grünewald, P., McDowall, W. and Ekins, P.** (2015). Hydrogen and fuel cell technologies for heating: A review, *International journal of hydrogen energy*, 40(5), 2065–2083.
- [18] **Shirley, C. and Gecan, R.** (2022). *Emissions of Carbon Dioxide in the Transportation Sector*, [\url{https://www.cbo.gov/system/files/2022-12/58566-co2-emissions-transportation.pdf}](https://www.cbo.gov/system/files/2022-12/58566-co2-emissions-transportation.pdf), accessed April 15, 2024.
- [19] **Larminie, J. and Dicks, A.** (2003). *Fuel Cell Systems Explained*, John Wiley & Sons Ltd, 2nd edition.
- [20] **Ulgiati, S.** (2003). Energy Flows in Ecology and in the Economy, *Encyclopedia of Physical Science and Technology*, 5, 441–460.
- [21] **Chan, S.H. and Wang, H.M.** (2000). Thermodynamic analysis of natural-gas fuel processing for fuel cell applications, *International Journal of Hydrogen Energy*, 25, 441–449.
- [22] **Center for Sustainable Systems, University of Michigan** (2023). *Hydrogen Factsheet*, <https://css.umich.edu/publications/factsheets/energy/hydrogen-factsheet>, accessed April 23, 2024.
- [23] **MathWorks** (2019). *Fuzzy PID Control with Type-2 Fuzzy Inference Systems*, <https://www.mathworks.com/help/fuzzy/fuzzy-pid-control-with-type-2-fis.html>, accessed April 22, 2024.

- [24] **Taskin, A. and Kumbasar, T.** (2015). An open source Matlab/Simulink toolbox for interval type-2 fuzzy logic systems, *2015 IEEE Symposium Series on Computational Intelligence*, IEEE, pp.1561–1568.





## CURRICULUM VITAE

**Name Surname: Ömer Burak Sarıçay**

### EDUCATION:

- **M.Sc.:** 2024, Istanbul Technical University, Faculty of Electrical and Electronics Engineering, Control and Automation Engineering.
- **B.Sc.:** 2021, Istanbul Technical University, Faculty of Mechanical Engineering, Mechanical Engineering.

### PROFESSIONAL EXPERIENCE AND REWARDS:

- 2022-2024 Systems Engineer, AVL Turkey Research and Engineering.
- 2021-2022 Design Engineer, Turkish Aerospace Industry.

### PUBLICATIONS, PRESENTATIONS AND PATENTS ON THE THESIS:

- **Sarıçay, B.** and Çalışkan, F. (2024). Optimized Power Control Strategy for a Proton Exchange Membrane Fuel Cell System, *3rd International Graduate Symposium*, 8-10 May, 2024 Istanbul, Turkey.

### OTHER PUBLICATIONS, PRESENTATIONS AND PATENTS:

- **Sarıçay, B.**, Oğuz, E. and Kılıç, M. (2024). Dynamic Modelling of a 2-kW Solid Oxide Fuel Cell System, *11th International Conference on Electrical and Electronics Engineering*, 22-24 April, 2024 Muğla, Turkey.